

# INTERACTIONS OF TURING AND HOPF BIFURCATIONS IN AN ADDITIONAL FOOD PROVIDED DIFFUSIVE PREDATOR-PREY MODEL\*

Xun Cao<sup>1</sup> and Weihua Jiang<sup>1,†</sup>

**Abstract** Complex spatiotemporal dynamics of a diffusive predator-prey system involving additional food supply to predator and intra-specific competition among predator, are investigated. We establish critical conditions of the occurrence of Turing instability, which are necessary and sufficient. Furthermore, we also establish conditions of the occurrence of codimension-2 Turing-Hopf bifurcation and Turing-Turing bifurcation, by exploring interactions of Turing bifurcations and Hopf bifurcation. For Turing-Hopf bifurcation, by analyzing normal form truncated to order 3 which are derived by applying normal form method, it is shown that under proper conditions, diffusive predator-prey system generates interesting spatial, temporal and spatiotemporal patterns, including a pair of spatially inhomogeneous steady states, a spatially homogeneous periodic solution and a pair of spatially inhomogeneous periodic solutions. And numerical simulations are also shown to support theory analysis. Moreover, it is found that proper intra-specific competition among predator helps generate complex spatiotemporal dynamics. And, proper additional food supply to predator helps control the population fluctuations of predator and prey, while large quantity and high quality of additional food supply will lead to the extinction of prey and make predator change the source of food, which finally destroy the ecosystem. These investigations might help understand complex spatiotemporal dynamics of predator-prey system involving additional food supply to predator and intra-specific competition among predator, and help conserve species in an ecosystem via supplying suitable additional food.

**Keywords** Diffusive predator-prey system, Turing instability, Turing-Hopf bifurcation, spatiotemporal patterns, additional food supply.

**MSC(2010)** 35B10, 35B32, 35B35, 35B36, 35K57.

## 1. Introduction

A functional response in ecology which is the intake rate of a consumer as a function of food density, has relation to the numerical response which is the reproduction rate of a consumer, see Holling [17]. That is to say, functional responses describe conflicts between predator and prey. Actually, competition for limited resources,

<sup>†</sup>the corresponding author. Email address:[jiangwh@hit.edu.cn](mailto:jiangwh@hit.edu.cn)(W. Jiang)

<sup>1</sup>Department of Mathematics, Harbin Institute of Technology, Harbin 150001, China

\*The authors were supported by the National Natural Science Foundation of China (No.11871176).

such as food, water, habitat, mates or any other resource which is required for survival, always exists among predator in the real world. Therefore, it is essential and practical to introduce intra-specific competition among predator into predator-prey systems, in order to better understand dynamics of natural populations for predator and prey.

By introducing intra-specific competition among predator, Bazykin et al. [2] investigated following predator-prey model,

$$\begin{cases} \frac{dx}{dt} = rx \left(1 - \frac{x}{K}\right) - \frac{mxy}{ax + c}, \\ \frac{dy}{dt} = \frac{emxy}{ax + c} - dy - hy^2, \end{cases} \quad (1.1)$$

where  $x$  and  $y$  represent population numbers of prey and predator, respectively. Later, by modifying functional response function in system (1.1), Pal et al. [23] and Sarwardi et al. [27] investigated global stability and Hopf bifurcation for delayed predator-prey systems with Holling type III response function and Beddington-DeAngelis response function, respectively. Furthermore, Camara et al. [3] and Guin et al. [13] investigated spatiotemporal patterns of diffusive predator-prey systems with ratio-dependent functional response respectively, by introducing diffusion into system (1.1). And, it was found that intra-specific competition among predator is one of the most convincing mechanisms for the spontaneous generation of patterns in a homogeneous environment. For more information about intra-specific competition among predator, see [3, 16, 23, 27, 28, 42].

What's more, supplying additional food for predator has been certified effective in controlling the populations of predator and prey, which plays a significant role in biological control. And in recent years, many experimentalists and theoreticians have concentrated on investigating dynamics of predator-prey models with additional food supply to predator. Incorporating habitat complexity, additional food supply and time delay, Sahoo and Poria [24] proposed following predator-prey system

$$\begin{cases} \frac{dx}{dt} = r \left(1 - \frac{x}{k}\right) - \frac{a(1-c)xy}{1 + \alpha\xi + a(1-c)hx}, \\ \frac{dy}{dt} = \frac{\theta a(1-c)(x(t-\tau) + \xi)y(t-\tau)}{1 + \alpha\xi + a(1-c)hx(t-\tau)} - dy, \end{cases} \quad (1.2)$$

where  $\alpha$  reflects the quality of additional food, and  $\xi$  represents the quantity of additional food. They investigated stability of coexistence equilibrium and bifurcated periodic solutions, and bifurcation direction of Hopf bifurcation applying normal form method, where time delay  $\tau$  is the bifurcation parameter. And, they found that additional food supply could control the fluctuations of population size.

Moreover, Ghorai and Poria [11] discussed spatiotemporal patterns of system (1.2) with diffusion and without habitat complexity, by investigating Hopf bifurcation and Turing bifurcation. Especially, it was demonstrated that spatiotemporal chaos can be controlled by supplying suitable additional food to predator, which is helpful for understanding complex spatiotemporal dynamics of population dynamical models in presence of additional food. See [4, 6, 10, 20, 24–26, 29, 32] for more information.

Since intra-specific competition and additional food supply both have influence on dynamics of predator-prey systems, then comes a question that whether supplying additional food to predator will help a predator-prey system with intra-specific

competition among predator generate new interesting dynamics. Taking into account the joint effects of Holling type II functional response, diffusion which reflects the facts that the distribution of species is generally spatially heterogeneous and therefore the species will migrate toward regions of lower population density to improve the possibility of survival, additional food and intra-specific competition among predator, as well as habitat complexity which reduces the probability of capturing a prey by reducing the searching efficiency of predator and affects the attack coefficient, we have following diffusive predator-prey system,

$$\begin{cases} \frac{\partial u}{\partial t} - d_1 \Delta u = ru \left(1 - \frac{u}{K}\right) - \frac{a(1-c)uv}{1 + \alpha\xi + a(1-c)hu}, & x \in \Omega, t > 0, \\ \frac{\partial v}{\partial t} - d_2 \Delta v = \frac{\theta a(1-c)(u + \xi)v}{1 + \alpha\xi + a(1-c)hu} - dv - gv^2, & x \in \Omega, t > 0, \\ \frac{\partial u}{\partial \nu} = \frac{\partial v}{\partial \nu} = 0, & x \in \partial\Omega, t > 0, \\ u(x, 0) = u_0(x) \geq 0, v(x, 0) = v_0(x) \geq 0, & x \in \Omega, \end{cases} \quad (1.3)$$

where  $u(x, t)$  and  $v(x, t)$  stand for the densities of prey and predator at location  $x \in \Omega$  and time  $t \geq 0$ , respectively. And domain  $\Omega$  with smooth boundary  $\partial\Omega$ , is bounded in  $\mathbb{R}$ .  $\nu$  is the outward unit normal vector of boundary  $\partial\Omega$ . The homogeneous Neumann boundary conditions indicate that predator-prey system is self-contained with zero population flux across the boundary. The positive constants  $d_1$  and  $d_2$  are diffusion coefficients, and the initial functions  $u_0(x)$  and  $v_0(x)$  are non-negative continuous functions. Moreover,  $K$  is the carrying capacity of the prey in ecosystem;  $\theta$  ( $0 < \theta < 1$ ) is the conversion efficiency of prey into the predator;  $a(1-c)$  is the attack coefficient, where  $c$  ( $0 < c < 1$ ) is a dimension less parameter, which measures the degree or strength of habitat complexity;  $h$  is the handling time per food item;  $\alpha$  represents the quality of additional food;  $\xi$  measures the quantity of additional food;  $r$  reflects prey intrinsic growth rate;  $d$  stands for predator death rate;  $g$  means predator interspecies competition. What's more, all parameters are positive, see [16, 25] to understand the meanings of these parameters in detail.

Since diffusive predator-prey systems with additional food supply or with intra-specific competition could produce complex temporal patterns and spatial patterns, we would like to know whether diffusive predator-prey system involving these two factors could generate more interesting and more complex spatiotemporal dynamics, like spatiotemporal patterns with spatial period and temporal period. Based on this idea, we explore spatiotemporal dynamics of diffusive system (1.3), by investigating codimension-2 Turing-Hopf bifurcation induced by interactions of Turing bifurcation and Hopf bifurcation.

It is worth noting that, codimension-2 bifurcations like Bogdanov-Takens bifurcation and fold-Hopf bifurcation, can induce complex dynamics, see [19, 22, 35, 44]. Similarly, codimension-2 Turing-Hopf bifurcation could also induce abundant interesting spatiotemporal patterns, which are frequently utilized to explain spatiotemporal phenomena in chemical reaction models, epidemic models, competition-cooperation models and predator-prey models, see [1, 3, 5, 7, 21, 33, 34, 36, 41, 43]. And, these complex spatiotemporal phenomena, like spatially inhomogeneous periodic solutions, might not be explained by Turing bifurcation and Hopf bifurcation. Moreover, these spatiotemporal phenomena with temporal period and spatial period are common in the real world. Therefore, it is necessary to investigate Turing-Hopf bi-

furcation and corresponding spatiotemporal dynamics, in order to better understand the mechanisms of the formation of some complex spatiotemporal patterns and to reveal some complex spatiotemporal phenomena. Ordinarily, normal form method is efficient in exploring dynamics of differential systems, see [8, 9, 14, 15, 31, 38]. And given that it is absolutely not easy to calculate normal forms, Jiang et al. [18] and Song et al. [30] recently derived several concise formulas of computing normal forms for partial functional differential equations and partial differential equations at Turing-Hopf singularity of codimension 2, respectively. Especially, these formulas can help one calculate normal forms more easily. Moreover, utilizing normal form method, Yang et al. [41], Xu et al. [39] and Song et al. [30] explored dynamics of diffusive predator-prey systems near Turing-Hopf singularity, respectively. It was found that diffusive systems generate numerous interesting multiple spatial, temporal and multiple spatiotemporal patterns through Turing-Hopf bifurcation.

Taking into account the joint effects of several factors, we investigate spatiotemporal dynamics of diffusive predator-prey system (1.3) involving additional food supply to predator and intra-specific competition among predator. By discussing characteristic equations of diffusive predator-prey system (1.3), we maximize parameter region for the stability of coexistence equilibrium, of which the boundary consists of Turing bifurcation curves and Hopf bifurcation curve. Meanwhile, we establish critical conditions of the occurrence of Turing instability, which are necessary and sufficient. Because that these critical conditions depend on spatial wave numbers, they could help determine spatial wavelength for a spatially inhomogeneous solution. Furthermore, by considering interactions of Turing bifurcations and Hopf bifurcation, we establish conditions of the occurrence of codimension-2 Turing-Hopf bifurcation and Turing-Turing bifurcation. For Turing-Hopf bifurcation, by analyzing normal form truncated to order 3, which is derived by applying normal form method [8] and concise formulas developed by Jiang et al. [18], we present bifurcation set and corresponding phase portraits for normal form restricted on center manifold at Turing-Hopf singularity. And, we find that system exhibits spatial, temporal and spatiotemporal patterns, like stable spatially homogeneous periodic solution, a pair of spatially inhomogeneous steady states and a pair of spatially inhomogeneous periodic solutions. Numerical simulations, including bistable pattern that a pair of spatially inhomogeneous periodic solutions coexist, are also shown to support theory analysis. Moreover, it is found that proper intra-specific competition among predator induces complex patterns which could be used to explain complex natural phenomena, while little intra-specific competition among predator and much intra-specific competition among predator will lead to the loss of complexity in the ecosystem. And, proper additional food supply to predator helps control spatiotemporal chaos and protect the ecosystem, while large quantity and high quality of additional food supply to predator brings a fatal strike to the ecosystem.

This paper is organized as follows. In Section 2, we establish conditions of the occurrence of Turing-Hopf bifurcation, Turing-Turing bifurcation, and maximize parameter region of the stability of coexistence equilibrium. Moreover, we also determine the critical Turing bifurcation curve and Turing instability curve in parameter plane. Then in Section 3, normal form up to order 3 of diffusive predator-prey system at Turing-Hopf singularity of codimension 2, is derived. Next in Section 4, by analyzing the normal form truncated to order 3, it is found that diffusive predator-prey system exhibits spatial, temporal and spatiotemporal dy-

namics. And, numerical simulations are shown to support theory analysis. Some discussions are also presented in this section. At last, conclusions are in Section 5.

## 2. Interactions of Turing bifurcations and Hopf bifurcation

Firstly, for the sake of convenience, we denote

$$\eta = \frac{a(1-c)}{r(1+\alpha\xi)}, \quad \beta = \frac{a(1-c)h}{1+\alpha\xi}, \quad \gamma = \frac{\theta a(1-c)}{1+\alpha\xi}.$$

Then, system (1.3) is simplified as follows,

$$\begin{cases} \frac{\partial u}{\partial t} - d_1 \Delta u = ru \left( 1 - \frac{u}{K} - \frac{\eta v}{1 + \beta u} \right), & x \in \Omega, t > 0, \\ \frac{\partial v}{\partial t} - d_2 \Delta v = \frac{\gamma(u + \xi)v}{1 + \beta u} - dv - gv^2, & x \in \Omega, t > 0, \\ \frac{\partial u}{\partial \nu} = \frac{\partial v}{\partial \nu} = 0, & x \in \partial\Omega, t > 0, \\ u(x, 0) = u_0(x) \geq 0, v(x, 0) = v_0(x) \geq 0, & x \in \Omega. \end{cases} \quad (2.1)$$

For system (2.1),  $E_0 = (0, 0)$  and  $E_1 = (K, 0)$  are always boundary equilibria, while  $E_2 = \left(0, \frac{\gamma\xi - d}{g}\right)$  is a boundary equilibrium for  $\gamma\xi - d > 0$ . However, we have great interest in dynamics near interior equilibria. Suppose that one of interior equilibria, if they exist, is denoted as  $E_* = (u_*, v_*)$ , where  $u_*, v_*$  are positive constants. Then,  $u_*, v_*$  satisfy following algebraic equations,

$$1 - \frac{u}{K} - \frac{\eta v}{1 + \beta u} = 0, \quad \frac{\gamma(u + \xi)}{1 + \beta u} - d - gv = 0.$$

And, we derive following equivalent cubic equation, which  $u_* \in (0, K)$  satisfies,

$$h(u) := u^3 \beta^2 g + u^2 \beta (2 - K\beta)g + u(\eta K(\gamma - d\beta) + (1 - 2K\beta)g) - K(\eta d + g - \eta\gamma\xi) = 0.$$

If and only if  $h(u) = 0$  has a positive root belonging to  $(0, K)$ , system (2.1) has a positive constant equilibrium  $E_*$ . Actually, system (2.1) might have more than one positive equilibrium, considering that  $h(u)$  is a cubic equation. Firstly, we numerically explore the number of positive equilibria of system (2.1) when system parameters vary. Similar to the work of Zhang et al. [45], we choose  $K = 50, \eta = 1, \beta = 0.8, \gamma = 0.4, d = 0.2, l = 1$  and  $\xi = 0.1, \xi = 0.7, \xi = 0.9$  respectively, and further choose  $g$  as bifurcation parameter, then we have following equilibrium bifurcation diagram Fig 1.

As shown in Fig 1, for different combinations of parameters  $\xi, g$ , system (2.1) could have no positive equilibrium, one positive equilibrium, two positive equilibria or three positive equilibria. Specifically, according to the blue curve in Fig 1, for  $\xi = 0.1$ , system (2.1) has one positive equilibrium when  $g < g_1 = 0.0264$  or  $g > g_2 = 0.0517$ , two when  $g = g_1$  or  $g = g_2$ , and three when  $g_1 < g < g_2$ . And at critical values  $g = g_1$  or  $g = g_2$ , saddle-node bifurcation occurs. For  $\xi = 0.7$ , system (2.1) has no positive equilibrium when  $g < g_1 = 0.0275$ , one when  $g > g_2 = 0.104$  or  $g = g_1$ , two when  $g_1 < g < g_0 = 0.080$  or  $g = g_2$ , and three when  $g_0 < g < g_2$ ,

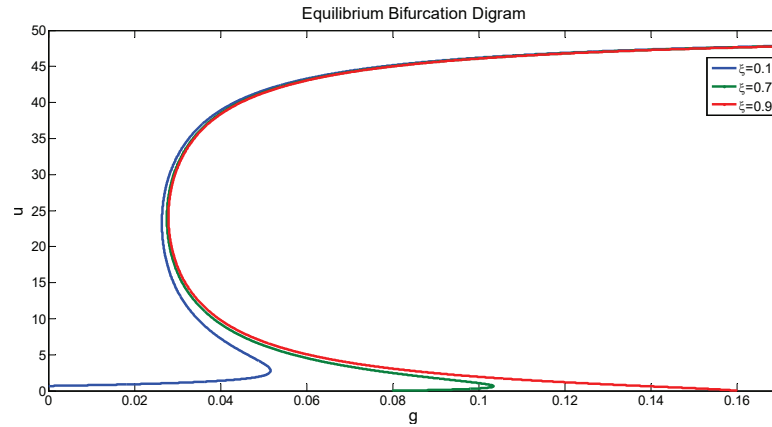


**Figure 1.** Equilibrium bifurcation:  $K = 50, \eta = 1, \beta = 0.8, \gamma = 0.4, d = 0.2, l = 1$  and  $\xi = 0.1, \xi = 0.7, \xi = 0.9$  respectively. And,  $g$  is bifurcation parameter. System (2.1) might have no positive equilibrium, one positive equilibrium, two positive equilibria or three positive equilibria, depending on different combinations of parameters  $\xi, g$ .

according to the green curve in Fig 1. Also, saddle-node bifurcation occurs at  $g = g_1$  or  $g = g_2$ . As for  $\xi = 0.9$ , system (2.1) has no positive equilibrium when  $g < g_1 = 0.0279$ , one when  $g = g_1$  or  $g > g_0 = 0.160$ , and two when  $g_1 < g < g_0$ , as shown by the red curve in Fig 1. At critical value  $g = g_1$ , saddle-node bifurcation occurs.

And, it is hard to provide some concise conditions to determine the exact number of positive equilibria. So in the following, we only establish the conditions of the existence of positive equilibria. And, we conclude that if

$$(H1) \quad (\eta d + g - \eta \gamma \xi) (\gamma(K + \xi) - d(1 + K\beta)) > 0,$$

system (2.1) has a positive constant equilibrium  $E_*$ , where  $u_* \in (0, K)$  and  $v_* = \frac{(K - u_*)(1 + \beta u_*)}{\eta K} > 0$ .

Thus, the linearized system of (2.1) at interior equilibrium  $E_*$  is

$$\begin{cases} \frac{\partial u}{\partial t} - d_1 \Delta u = r\alpha_1(u - u_*) - r\beta_1(v - v_*), \\ \frac{\partial v}{\partial t} - d_2 \Delta v = \alpha_2(u - u_*) - \beta_2(v - v_*), \end{cases} \tag{2.2}$$

where

$$\begin{aligned} \alpha_1 &= u_* \left( \frac{\eta \beta v_*}{(1 + \beta u_*)^2} - \frac{1}{K} \right), & \beta_1 &= \frac{\eta u_*}{1 + \beta u_*} > 0, \\ \alpha_2 &= \frac{\gamma v_*(1 - \beta \xi)}{(1 + \beta u_*)^2}, & \beta_2 &= g v_* > 0. \end{aligned} \tag{2.3}$$

Let  $\Omega = (0, l\pi), l > 0$ . Then, system (2.2) could be written as an abstract differential equation in the phase space  $X$  of the form

$$\begin{pmatrix} u_t \\ v_t \end{pmatrix} = L \begin{pmatrix} u \\ v \end{pmatrix} := D \begin{pmatrix} u_{xx} \\ v_{xx} \end{pmatrix} + J \begin{pmatrix} u \\ v \end{pmatrix}, \tag{2.4}$$

where  $X$  is the real-valued Sobolev space,

$$X := \left\{ (u, v)^T \in (W^{2,2}(0, l\pi))^2, \frac{\partial u}{\partial x} \Big|_{x=0, l\pi} = \frac{\partial v}{\partial x} \Big|_{x=0, l\pi} = 0 \right\},$$

which becomes a Hilbert space when we define the following inner product,

$$[U_1, U_2] = \int_0^{l\pi} (u_1 u_2 + v_1 v_2) dx, \quad U_1 = (u_1, v_1)^T \in X, U_2 = (u_2, v_2)^T \in X.$$

Moreover,

$$D = \begin{pmatrix} d_1 & 0 \\ 0 & d_2 \end{pmatrix}, \quad J = \begin{pmatrix} r\alpha_1 - r\beta_1 \\ \alpha_2 & -\beta_2 \end{pmatrix}.$$

Hence, characteristic equations of system (2.4) are

$$\Delta_k(\lambda) := \lambda^2 - T(k)\lambda + D(k) = 0, \quad k \in \mathbb{N}_0 \triangleq \mathbb{N} \cup \{0\}, \quad (2.5)$$

where  $\mathbb{N}$  is the natural set, and

$$T(k) := r\alpha_1 - \beta_2 - (d_1 + d_2) \frac{k^2}{l^2},$$

$$D(k) := r(\alpha_2\beta_1 - \alpha_1\beta_2) - (d_2 r\alpha_1 - d_1\beta_2) \frac{k^2}{l^2} + d_1 d_2 \frac{k^4}{l^4}.$$

Here are some important results, which we need in later discussions.

**Lemma 2.1.** *Assume that (H1) holds. If  $\alpha_1 > 0$  and*

$$(H2) \quad \Theta := \alpha_2\beta_1 - \alpha_1\beta_2 > 0,$$

*Hopf bifurcation occurs for system (2.1) at  $E_*$  when  $r = r_0$ , where*

$$r_0 := \frac{\beta_2}{\alpha_1}. \quad (2.6)$$

**Proof.** As we know, if  $T(0) = 0$  and  $D(0) > 0$ , characteristic equation (2.5) has a pair of pure imaginary roots. And considering that (H2) holds,  $D(0) > 0$  is obvious. Then let  $T(0) = 0$ , that is,  $r\alpha_1 - \beta_2 = 0$ , and we derive

$$r = r_0 := \frac{\beta_2}{\alpha_1}, \quad \text{for } \alpha_1 > 0.$$

Moreover, let  $\lambda(r) = \alpha(r) \pm i\omega(r)$  be a pair of complex roots of characteristic equation (2.5) when  $r$  is near  $r_0$ , then

$$\alpha(r) = \frac{T(0)}{2}, \quad \omega(r) = \sqrt{D^2(0) - 4T(0)},$$

with  $\alpha(r_0) = 0$  and  $\omega(r_0) > 0$ . Furthermore, we have

$$\frac{d\alpha(r)}{dr} \Big|_{r=r_0} = \frac{\alpha_1}{2} > 0,$$

which indicates that transversality condition holds. Thus according to Poincaré-Andronov-Hopf Bifurcation Theorem [37], system (2.1) undergoes Hopf bifurcation as  $r$  crosses through  $r_0$ .  $\square$

Then, we investigate interactions of Turing bifurcation and Hopf bifurcation, that is, the existence of Turing-Hopf bifurcation under the assumption (H1). As we know, if there exist a positive integer  $k_1$  and a nonnegative integer  $k_2$  such that  $\Delta_{k_1}(\lambda) = 0$  has a simple zero root and  $\Delta_{k_2}(\lambda) = 0$  has a pair of pure imaginary roots, and other roots of equations (2.5) have non-zero real part, and the transversality conditions hold, then we call the codimension-2 bifurcation as a  $(k_1, k_2)$ -mode Turing-Hopf bifurcation, see [18].

Actually, we discuss the existence of Turing-Hopf bifurcation, from a geometric point of view. We regard codimension-2 Turing-Hopf bifurcation point as the intersection of codimension-1 Turing bifurcation curve and codimension-1 Hopf bifurcation curve in parameter plane. And, we have following conclusions.

**Theorem 2.1.** *Assume (H1) holds. We have following results:*

1. *If (H2) holds and  $\alpha_1 > 0$ , system (2.1) undergoes Hopf bifurcation at  $r = r_0$ ; Otherwise if  $\alpha_1 \leq 0$ , system (2.1) doesn't exhibit Hopf bifurcation.*
2. *If  $\Theta < 0$  or  $\alpha_1 > 0$ , system (2.1) undergoes Turing bifurcation at  $r = r_k(d_2)$  for  $\alpha_1 d_2 \frac{k^2}{l^2} - \Theta > 0, k \in \mathbb{N}$ ; Otherwise, system doesn't exhibit Turing bifurcation.*
3. *If (H2) holds,  $\alpha_1 > 0$  and  $d_1 < \beta_2 l^2$ , system (2.1) exhibits  $(k, 0)$ -mode Turing-Hopf bifurcation at  $(u_*, v_*)$  when  $(d_2, r) = (d_k^*, r_0), 1 \leq k \leq k^* := \left\lceil \sqrt{\frac{\beta_2}{d_1} l} \right\rceil - 1$ , where  $\lceil \cdot \rceil$  stands for the ceiling function; Otherwise, Turing-Hopf bifurcation doesn't occur for system (2.1), where*

$$r_k(d_2) := \frac{d_1 \left( \beta_2 + d_2 \frac{k^2}{l^2} \right) \frac{k^2}{l^2}}{-\Theta + \alpha_1 d_2 \frac{k^2}{l^2}}, \quad k \in \mathbb{N},$$

$$d_k^* = \frac{\beta_2 \left( \Theta + \alpha_1 d_1 \frac{k^2}{l^2} \right)}{\alpha_1 \left( \beta_2 - d_1 \frac{k^2}{l^2} \right) \frac{k^2}{l^2}}, \quad k \in [1, k^*].$$

**Proof.**

1. According to Lemma 2.1, the conclusion is obvious. Then  $\Delta_0(\lambda) = 0$  has a pair of simple pure imaginary roots at  $r = r_0$ , which is denoted as  $\mathcal{H}_0$  in  $d_2$ - $r$  plane, that is

$$\mathcal{H}_0 : r = r_0.$$

Actually,  $\mathcal{H}_0$  is Hopf bifurcation curve in  $d_2$ - $r$  plane.

However, if  $\alpha_1 \leq 0$ , then

$$T(k) := r\alpha_1 - \beta_2 - (d_1 + d_2) \frac{k^2}{l^2} < 0, \quad \forall k \in \mathbb{N}_0,$$

thus Hopf bifurcation doesn't occur for diffusive system (2.1), which indicates that system (2.1) doesn't exhibit Turing-Hopf bifurcation.

2. Let  $\Delta_k(0) = 0$ ,  $k \in \mathbb{N}$ , then

$$r\Theta - (d_2 r \alpha_1 - d_1 \beta_2) \frac{k^2}{l^2} + d_1 d_2 \frac{k^4}{l^4} = 0.$$

Thus we derive

$$r = r_k(d_2) := \frac{d_1 \left( \beta_2 + d_2 \frac{k^2}{l^2} \right) \frac{k^2}{l^2}}{\alpha_1 d_2 \frac{k^2}{l^2} - \Theta}, \quad k \in \mathbb{N}. \quad (2.7)$$

Hence, if  $\Theta < 0$  or  $\alpha_1 > 0$ , then  $r_k(d_2) > 0$  for proper parameters. Hence, system (2.1) undergoes Turing bifurcation at  $r = r_k(d_2)$ . Otherwise, if  $\Theta > 0$  and  $\alpha_1 < 0$ , then  $r_k < 0$ . Therefore, system (2.1) doesn't exhibit Turing bifurcation, which indicates that system (2.1) doesn't undergo Turing-Hopf bifurcation.

3. A direct calculation yields,

$$\frac{dr_k(d_2)}{dd_2} = -\frac{d_1 \alpha_2 \beta_1 \frac{k^4}{l^4}}{\left( \alpha_1 d_2 \frac{k^2}{l^2} - \Theta \right)^2} < 0, \quad \text{for } \alpha_2 > 0, \quad (2.8)$$

which indicates that  $r_k(d_2)$  monotonically decreases in  $d_2$ . Actually,  $\alpha_2 > 0$  is obvious, for  $\Theta > 0$  and  $\alpha_1 > 0$ .

And, Turing bifurcation curve in  $d_2$ - $r$  plane is denoted as  $\mathcal{L}_k$ , where

$$\mathcal{L}_k : r = r_k(d_2), \quad d_2 > d_{2,k} := \frac{\Theta l^2}{\alpha_1 k^2}, \quad k \in \mathbb{N}.$$

According to equation (2.7), we need  $d_2 > d_{2,k}$ ,  $k \in \mathbb{N}$  to guarantee the positivity of  $r_k(d_2)$ .

Furthermore, we have  $\lim_{d_2 \rightarrow \infty} r_k(d_2) = \frac{d_1 k^2}{\alpha_1 l^2}$ . If  $\frac{d_1}{\alpha_1 l^2} \geq r_0$ , then  $r_k(d_2) > r_0, \forall k \in \mathbb{N}$  for  $d_2 > d_{2,k}$ , considering the monotonicity of  $r_k(d_2)$ . Then, Turing bifurcation curve doesn't intersect with Hopf bifurcation curve, which indicates that system doesn't undergo Turing-Hopf bifurcation.

And  $\lim_{d_2 \rightarrow \infty} r_k(d_2) = \frac{d_1 k^2}{\alpha_1 l^2} < r_0$  when  $k \leq k^* = \left\lceil \sqrt{\frac{\beta_2 l}{d_1}} \right\rceil - 1$ , where  $\lceil \cdot \rceil$  is the ceiling function, and  $r_k(d_2) > r_0$  for small enough  $d_2 > d_{2,k}$ ,  $k \in \mathbb{N}$ . Therefore, there exists a  $d_2^*$  satisfying  $r_k(d_2^*) = r_0$ . Moreover,  $k^* \geq 1$ , since  $d_1 < \beta_2 l^2$  which indicates that  $\lim_{d_2 \rightarrow \infty} r_1(d_2) < r_0$ . Thus, the intersection  $(d_k^*, r_0)$  of  $\mathcal{H}_0$  and  $\mathcal{L}_k$  exists for  $1 \leq k \leq k^*$ . Moreover, according to equation (2.8),  $r_k(d_2)$  is monotonically decreasing in  $d_2$ , which indicates that there exists a unique intersection between  $\mathcal{L}_k$  and  $\mathcal{H}_0$  for each  $k \in [1, k^*]$ . And we denote the unique intersection of  $\mathcal{H}_0$  and  $\mathcal{L}_k$  by  $(d_k^*, r_0)$ , where

$$d_k^* = \frac{\beta_2 \left( \Theta + \alpha_1 d_1 \frac{k^2}{l^2} \right)}{\alpha_1 \left( \beta_2 - d_1 \frac{k^2}{l^2} \right) \frac{k^2}{l^2}}. \quad (2.9)$$

To ensure  $d_k^* > 0$ , we need  $\beta_2 - d_1 \frac{k^2}{l^2} > 0$ , i.e.  $k \leq k^*$ . Then  $d_k^* > 0, r_k^* > 0$  for  $1 \leq k \leq k^*$ .

Moreover, assume  $\lambda_1(r) = \alpha_1(r) + i\beta_1(r)$  with  $\alpha_1(r_0) = 0, \beta_1(r_0) = \omega > 0$ , and  $\lambda_2(r) = \alpha_2(r) + i\beta_2(r)$  with  $\alpha_2(r_k(d_2)) = 0, \beta_2(r_k(d_2)) = 0$ , then the transversality conditions are as follows:

$$\begin{aligned} \frac{d\Re(\lambda_1(r))}{dr} \Big|_{r=r_0} &= \frac{\alpha_1}{2} > 0, \\ \frac{d\Re(\lambda_2(r))}{dr} \Big|_{r=r_k(d_2)} &= \frac{-2\Theta + 3\alpha_1 d_2 \frac{k^2}{l^2}}{-T(k)} > \frac{\Theta}{-T(k)} > 0, \quad \text{for } 0 < r < r_0, \end{aligned}$$

where  $\Re(z)$  stands for the real part of complex number  $z$ .

Then, the conclusions follow. □

What's more, let  $l_k = \frac{dr_k(d_2)}{dd_2} < 0$ , then

$$\begin{aligned} \frac{dl_k}{dk} &= \frac{-4d_1\alpha_2\beta_1(\alpha_1\beta_2 - \alpha_2\beta_1)\frac{k^3}{l^4}}{(\alpha_1\beta_2 - \alpha_2\beta_1 + \alpha_1d_2\frac{k^2}{l^2})^3} > 0, \\ \frac{dl_k}{dd_2} &= \frac{2d_1\alpha_2\beta_1\alpha_1\frac{k^6}{l^6}}{(\alpha_1\beta_2 - \alpha_2\beta_1 + \alpha_1d_2\frac{k^2}{l^2})^3} > 0, \quad d_2 > d_{2,k}, \end{aligned}$$

which means that  $l_k$  monotonically increases in  $k$  and  $d_2$ , that is, the slope of curve  $\mathcal{L}_k$  monotonically increases as  $k$  increases in turn.

Similarly, we have following conclusion of the interactions of Turing bifurcation- $s$ , that is, codimension-2 Turing-Turing bifurcation. As we know, Turing-Turing bifurcation is degenerated Turing bifurcation. And Turing-Turing bifurcation point could also be regarded as the intersection of two Turing bifurcation curves  $\mathcal{L}_k$  with different wave numbers  $n$  and  $n_0$ , see [40, 41].

**Theorem 2.2.** *Assume that (H1) and (H2) hold. If  $\alpha_1 > 0$ , system (2.1) undergoes codimension-2  $(i, j)$ -mode Turing-Turing bifurcation at  $(u_*, v_*)$  when  $(d_2, r) = (d_{i,j}^*, r_{i,j}^*)$ , where*

$$\begin{aligned} d_{i,j}^* &= \frac{\Theta r_{i,j}^* + \beta_2 d_1 \frac{i^2}{l^2}}{\frac{i^2}{l^2} (\alpha_1 r_{i,j}^* - d_1 \frac{i^2}{l^2})} > 0, \quad i, j \in \mathbb{N}, \\ r_{i,j}^* &= \frac{d_1 \Theta (i^2 + j^2) + d_1 \sqrt{\Theta^2 (i^2 + j^2)^2 + 4\beta_2^2 i^2 j^2 \alpha_1 \Theta}}{2\alpha_1 \Theta l^2} > 0. \end{aligned}$$

**Proof.** Here, we prove this theorem in two steps.

1. For  $i, j \in \mathbb{N}$ , let  $j > i$ , then Turing curve  $\mathcal{L}_j$  intersects with curve  $\mathcal{L}_i$  in the first quadrant in  $d_2$ - $r$  plane. Firstly, we have

$$\lim_{d_2 \rightarrow \infty} r_k(d_2) = \frac{d_1 k^2}{\alpha_1 l^2},$$

obviously  $\lim_{d_2 \rightarrow \infty} r_k(d_2) > 0$  monotonically increases in  $k$ , thus there exists a large enough  $d_2^* > 0$  satisfying  $r_k(d_2^*) > 0$  monotonically increases in  $k$ , i.e.  $r_j(d_2^*) > r_i(d_2^*)$ . Moreover,  $r_k(d_2) \geq 0$  for  $d > d_{2,k}$ . Therefore,  $d_{2,j} < d_{2,i}$ . Thus, there exists a small enough  $\varepsilon$  satisfying  $r_i(d_{2,i} + \varepsilon) > r_j(d_{2,i} + \varepsilon)$ .

Define function  $d(d_2) = r_j(d_2) - r_i(d_2)$  with the domain being  $[d_{2,i} + \varepsilon, d_2^*]$ , then  $d(d_{2,i} + \varepsilon) = r_j(d_{2,i} + \varepsilon) - r_i(d_{2,i} + \varepsilon) < 0$ ,  $d(d_2^*) = r_j(d_2^*) - r_i(d_2^*) > 0$ . According to *Intermediate Value Theorem*, there is a  $d_{ij}^*$  satisfying  $d(d_{ij}^*) = 0$ , i.e.  $r_j(d_{ij}^*) = r_i(d_{ij}^*)$ . And we easily obtain  $r_{ij}^* = r_j(d_{ij}^*)$ .

- There is only one intersection. We consider the monotonicity of  $d(d_2) = r_j(d_2) - r_i(d_2)$ , thus

$$\frac{dd(d_2)}{dd_2} = \frac{dr_j(d_2)}{dd_2} - \frac{dr_i(d_2)}{dd_2} = l_j - l_i > 0, \quad \text{for } d_2 \in [d_{2,i} + \varepsilon, d_2^*],$$

since  $l_k$  monotonically increases in  $k$ . Therefore, there exists a unique  $d_{ij}^*$  satisfying  $d(d_{ij}^*)=0$ , that is, there is only one intersection between  $\mathcal{L}_j$  and  $\mathcal{L}_i$ .

Therefore, the unique intersection between  $\mathcal{L}_i$  and  $\mathcal{L}_j$  is denoted as  $(d_{i,j}^*, r_{i,j}^*)$ , where  $r_{i,j}^*$  satisfies following equation

$$\alpha_1 \Theta \left( \frac{rl^2}{d_1} \right)^2 - \Theta(i^2 + j^2) \frac{rl^2}{d_1} - \beta_2 i^2 j^2 = 0.$$

Thus, we obtain a negative root which should be abandoned, and a positive root

$$r_{i,j}^* = \frac{d_1 \Theta(i^2 + j^2) + d_1 \sqrt{\Theta^2(i^2 + j^2)^2 + 4\beta_2 i^2 j^2 \alpha_1 \Theta}}{2\alpha_1 \Theta l^2} > 0.$$

And substituting  $r_{i,j}^*$  into  $\Delta_j(0) = 0$ , we attain  $d_{i,j}^*$ . Therefore, system (2.1) undergoes  $(i, j)$ -mode Turing-Turing bifurcation at  $(d_{i,j}^*, r_{i,j}^*)$ .  $\square$

However, we are more interested in some special Turing-Hopf bifurcation point and Turing-Turing bifurcation points, with the remaining eigenvalues having negative real parts. We firstly determine the unique special Turing-Hopf bifurcation point.

**Theorem 2.3.** *If (H1) and (H2) hold,  $\alpha_1 > 0$  and  $d_1 < \beta_2 l^2$ , system (2.1) undergoes  $(k_0^*, 0)$ -mode Turing-Hopf bifurcation, with real parts of all roots of characteristic equations (2.5) being negative except a simple zero root and a pair of pure imaginary roots, only when  $(d_2, r) = (d_{k_0^*}^*, r_0)$ , where*

$$k_0^* = \min \{l : d_l^* = \min d_k^*, k \in [1, k^*]\}.$$

**Proof.** In order to determine the unique special Turing-Hopf bifurcation point, we calculate the derivation of  $d_k^*$  in  $k$ ,

$$\frac{dd_k^*}{dk} = \frac{2\beta_2 \frac{k^2}{l^2} \left( \alpha_1 d_1^2 \frac{k^4}{l^4} + 2\Theta d_1 \frac{k^2}{l^2} - \Theta \beta_2 \right)}{\alpha_1 \frac{k^3}{l^2} \left( \beta_2 - d_1 \frac{k^2}{l^2} \right)^2}.$$

And, we need to determine the sign of  $\frac{dd_k^*}{dk}$ . Obviously,  $\frac{dd_k^*}{dk}$  has the same sign with  $\varphi\left(\frac{k^2}{l^2}\right) = \alpha_1 d_1^2 \left(\frac{k^2}{l^2}\right)^2 + 2\Theta d_1 \frac{k^2}{l^2} - \Theta \beta_2$ , since  $\alpha_1, \beta_2$  are positive. Next, we focus on discussing the sign of  $\varphi\left(\frac{k^2}{l^2}\right)$ . Let  $\varphi(x) = \alpha_1 d_1^2 x^2 + 2\Theta d_1 x - \Theta \beta_2$  for  $x \geq 0$ , and

$\lim_{x \rightarrow 0^+} \varphi(0) = -\Theta\beta_2 < 0$ ,  $\lim_{x \rightarrow +\infty} \varphi(x) = +\infty$ . Thus, there exists a unique positive  $x_*$  satisfying  $\varphi(x_*) = 0$ , and  $\varphi(x)$  is negative in interval  $[0, x_*)$ . We denote

$$k_m^0 := \lfloor \sqrt{x_*}l \rfloor = \left\lfloor \sqrt{\frac{-\Theta + \sqrt{\Theta^2 + \alpha_1\beta_2\Theta}}{\alpha_1 d_1}} l \right\rfloor,$$

where  $\lfloor \cdot \rfloor$  is the floor function. And for  $k_m = \max\{1, \min\{k_m^0, k^*\}\}$ ,  $d_k^*$  monotonically decreases in interval  $[1, k_m]$  for  $k_m > 1$ , and monotonically increases in interval  $[k_m + 1, k^*]$  for  $k_m + 1 < k^*$  in  $k$ .

We also denote

$$k_0^* = \begin{cases} 1, & \text{if } k_m = 1; \\ k^*, & \text{if } k_m = k^*; \\ k_m, & \text{if } d_{k_m}^* < d_{k_m+1}^*, k^* > k_m > 1; \\ k_m + 1, & \text{if } d_{k_m}^* > d_{k_m+1}^*, k^* > k_m > 1. \end{cases}$$

Then for  $k_0^*$  given above, we know that  $d_{k_0^*} = \min_{1 \leq k \leq k^*} \{d_k\}$ .

Actually, reaction-diffusion system (2.1) undergoes Turing-Turing-Hopf bifurcation which is a codimension-3 bifurcation, when  $d_{k_m}^* = d_{k_m+1}^*$ . And we won't consider this kind of bifurcation for the time being.

Thus, the Hopf bifurcation curve  $\mathcal{H}_0$  intersects with Turing bifurcation curve  $\mathcal{L}_{k_0^*}$  at  $(d_{k_0^*}, r_0)$ , which is the  $(k_0^*, 0)$ -mode Turing-Hopf bifurcation point, with real parts of the remaining roots of  $\Delta_k(\lambda) = 0$  ( $k \neq k_1, k_2$ ) being negative.

Moreover, the transversality conditions are obvious, according to Theorem 2.1. So, we prove the theorem.  $\square$

However, it is difficult to determine these special Turing-Turing points which we have great interest in. But, we claim that these special points locate on boundary of parameter region of the stability for coexistence equilibrium. Next, we would like to make further efforts to determine parameter region of the stability for coexistence equilibrium and critical curve of Turing instability which makes up right boundary of the parameter region.

To determine the maximal parameter region of the stability for coexistence equilibrium, we firstly give following lemmas.

**Lemma 2.2.** *Assume (H1) and (H2) hold, and  $k_0^* \geq 2$ . For  $1 \leq i, j \leq k_0^*$ ,  $\mathcal{L}_i$  and  $\mathcal{L}_j$  intersect when  $r < r_0$ , that is, the intersection of Turing bifurcation curves  $\mathcal{L}_i$  and  $\mathcal{L}_j$  is below the Hopf bifurcation curve  $\mathcal{H}_0$ .*

**Proof.** We prove this lemma by the contradictory. Assume that the intersection  $(d_{i,j}^*, r_{i,j}^*)$  is above curve  $\mathcal{H}_0$  in  $d_2$ - $r$  plane. Let  $j > i \geq 1$ , then  $d_{i,j}^* < d_j^* < d_i^*$ . Based on *Newton-Leibniz Formula*, we derive

$$r_0 - r_{i,j}^* = \int_{d_{i,j}^*}^{d_j^*} l_j dd_2 = \int_{d_{i,j}^*}^{d_i^*} l_i dd_2 = \int_{d_{i,j}^*}^{d_j^*} l_i dd_2 + \int_{d_j^*}^{d_i^*} l_i dd_2,$$

which is contradictory since  $l_i < l_j < 0$  for all  $d_2 \in (d_{i,j}^*, d_j^*)$ , and  $d_i^* > d_j^*$  because  $d_k^*$  decreases in  $k$ .  $\square$

**Lemma 2.3.** *Assume (H1) and (H2) hold. For  $i, j \geq k_0^*$ ,  $\mathcal{L}_i$  and  $\mathcal{L}_j$  intersect when  $r > r_0$ , that is, the intersection of Turing bifurcation curves  $\mathcal{L}_i$  and  $\mathcal{L}_j$  is above the Hopf bifurcation curve  $\mathcal{H}_0$ .*

**Proof.** Let  $i < j$ . We firstly prove that there is an intersection above  $\mathcal{H}_0$  between  $\mathcal{L}_i$  and  $\mathcal{L}_j$ , applying *Intermediate Value Theorem*. Since the proof is similar to proof of Theorem 2.2, we omit it here.

Then, the intersection is above curve  $\mathcal{H}_0$ , considering the uniqueness of intersection between  $\mathcal{L}_i$  and  $\mathcal{L}_j$ .  $\square$

Based on Lemma 2.2 and 2.3, we have following conclusion.

**Theorem 2.4.** *Assume (H1) and (H2) hold. If  $\alpha_1 > 0$  and  $d_1 < \beta_1 l^2$ , the coexistence equilibrium  $E_*$  is stable for  $(d_2, r) \in \mathcal{U}$ , where*

$$\mathcal{U} = \left\{ (d_2, r) \mid 0 < r < r_0, \text{ if } 0 < d_2 \leq d_{k_0}^*, \text{ and } 0 < r < r_T, \text{ if } d_2 > d_{k_0}^* \right\},$$

with

$$\mathcal{T} : r_T = \begin{cases} r_k, & \text{if } d_{k,k+1}^* < d_2 \leq d_{k-1,k}^*, k > 1, \\ r_1, & \text{if } d_2 > d_{1,2}^*, k = 1, \end{cases}$$

and  $d_{k-1,k}^*$ ,  $k \geq 2$  is the intersection of Turing bifurcation curves  $\mathcal{L}_{k-1}$  and  $\mathcal{L}_k$ . Moreover,  $\mathcal{T}$  is the critical curve. Diffusive system (2.1) undergoes Turing bifurcation for the first time, when bifurcation parameter point  $(d_2, r)$  crosses through  $\mathcal{T}$  in  $d_2$ - $r$  plane. Furthermore, the part of curve  $\mathcal{T}$ , which is below  $\mathcal{H}_0$ , is also called the critical Turing instability curve (see Figure 2).

**Proof.** According to Lemma 2.3, the curve  $\mathcal{L}_k$  is above the curve  $\mathcal{L}_{k_0}^*$  for  $k \geq k_0^*$ , since they don't intersect below Hopf bifurcation curve  $\mathcal{H}_0$ . And there is a unique intersection  $(d_{i,j}^*, r_{i,j}^*)$  between curves  $\mathcal{L}_i$  and  $\mathcal{L}_j$  for  $j > i$ . According to Theorem 2.2,

$$r_{i,j}^* = \frac{d_1 \Theta (i^2 + j^2) + d_1 \sqrt{\Theta^2 (i^2 + j^2)^2 + 4\beta_2^2 i^2 j^2 \alpha_1 \Theta}}{2\alpha_1 \Theta l^2}.$$

Then, a direct calculation yields,

$$\frac{dr_{i,j}^*}{di} > 0, \quad \frac{dr_{i,j}^*}{dj} > 0,$$

which represents that  $r_{i,j}^*$  monotonously increases in  $i, j$ , respectively.

Moreover,  $d_{i,j}^*$  monotonically decreases in  $i, j$  respectively, given the monotonicity of  $r_k(d_2)$  in  $d_2$ .

Therefore,  $d_{k,k+1}^* < d_{k-1,k+1}^* < d_{k-1,k}^*$  and  $r_{k,k+1}^* > r_{k-1,k+1}^* > r_{k-1,k}^*$  for  $k > 1$ . Thus, bifurcation curves  $\mathcal{L}_{k-1}$ ,  $\mathcal{L}_{k+1}$  and bifurcation point  $(d_{k-1,k+1}^*, r_{k-1,k+1}^*)$  are above bifurcation curve  $\mathcal{L}_k$ , when  $d_2 \in (d_{k,k+1}^*, d_{k-1,k}^*)$ .

Then, the coexistence equilibrium is stable for  $0 < d_2 \leq d_{k_0}^*, 0 < r < r_0$ , since bifurcation parameter point  $(d_2, r)$  doesn't cross through the Hopf bifurcation curve  $\mathcal{H}_0$ ; analogously, bifurcation parameter point  $(d_2, r)$  doesn't cross through the Turing bifurcation curve  $\mathcal{L}_k$ ,  $k \in \mathbb{N}$  when  $d_2 > d_{k_0}^*, 0 < r < r_T$ . Therefore, the coexistence equilibrium is stable.

In summary, the coexistence equilibrium  $(u_*, v_*)$  of reaction-diffusion system (2.1) is stable, when parameter point  $(d_2, r)$  is below bifurcation curves  $\mathcal{T}$  and  $\mathcal{H}_0$ , that is,  $(d_2, r) \in \mathcal{U}$ .  $\square$

Then, according to Theorem 2.2 and 2.4, we could determine these special Turing-Turing bifurcation points, which satisfy that characteristic equations of

reaction-diffusion system have two independent zero roots with the remaining roots having negative real parts.

**Theorem 2.5.** *Assume that conditions in Theorem 2.2 hold. For  $k_0^* \geq k \geq 2$ ,  $(k-1, k)$ -mode Turing-Turing bifurcation points  $(d_{k-1,k}^*, r_{k-1,k}^*)$  are locating on boundary of parameter region of the stability for coexistence equilibrium, satisfying that characteristic equations (2.5) have two independent zero roots with the remaining roots having negative real parts.*

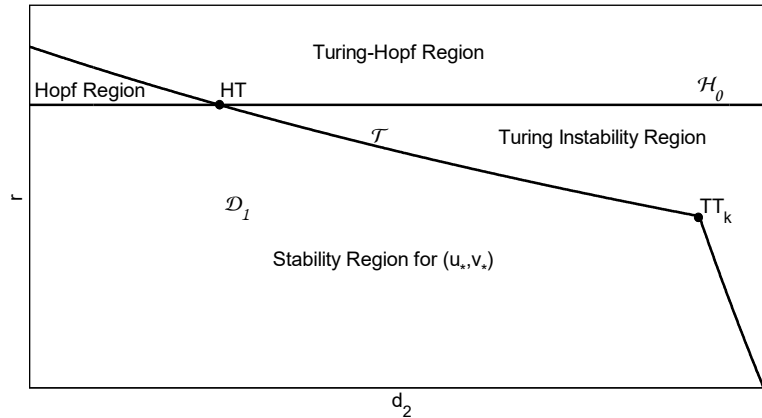


**Figure 2.** Parameter region of the stability for coexistence equilibrium, and bifurcation curves in  $d_2$ - $r$  plane. And  $HT$  stands for  $(k_0^*, 0)$ -mode Turing-Hopf bifurcation point  $(d_{k_0^*}^*, r_0)$ . Moreover,  $TT_k$  represents  $(k, k+1)$ -mode Turing-Turing bifurcation point  $(d_{k,k+1}^*, r_{k,k+1}^*)$  for  $k \in \mathbb{N}$ , which locates on the critical Turing bifurcation curve  $\mathcal{T}$ .

**Remark 2.1.** In this paper, we determine parameter region  $\mathcal{D}_1$  of the stability for coexistence equilibrium  $E_{**}$ , as large as possible, see Figure 2.

**Remark 2.2.** We could easily determine the spatial wavelength for a spatially inhomogeneous solution of diffusive system (2.1), when parameter point  $(d_2, r)$  is chosen near the critical Turing bifurcation curve  $\mathcal{T}$ , since the critical Turing bifurcation curve has relation to spatial wave numbers.

And, in Figure 2, we see that system (2.1) undergoes Hopf bifurcation and generates a spatially homogeneous periodic solution, when parameters cross through Hopf bifurcation curve  $\mathcal{H}_0$  and reach Hopf region. Analogously, system (2.1) undergoes Turing bifurcation and produces a pair of spatially inhomogeneous steady states when parameters cross through the critical Turing instability curve and reach Turing instability region. However, when parameters cross through Hopf bifurcation curve  $\mathcal{H}_0$  and critical Turing bifurcation curve  $\mathcal{T}$  and reach Turing-Hopf region, that is, system (2.1) undergoes Turing-Hopf bifurcation, dynamical behaviors of system (2.1) are still unknown. Then a question arises:

- Near Turing-Hopf bifurcation point, what are dynamical behaviors of diffusive system (2.1) when parameter point  $(d_2, r)$  is chosen in Hopf region, Turing region and Turing-Hopf region, respectively?

And in next two sections, we discuss dynamics of system (2.1) and answer the

question, utilizing normal form method and numerical tools.

### 3. Normal form of Turing-Hopf bifurcation

In this part, we calculate normal form of reaction-diffusion system (2.1) at Turing-Hopf singularity. Firstly by letting  $d_2 = d_{k_0^*}^* + \mu_1, r = r_0 + \mu_2$ , we introduce perturbation parameters  $\mu_1, \mu_2$ , which satisfy that reaction-diffusion system (2.1) undergoes  $(k_0^*, 0)$ -mode Turing-Hopf bifurcation at the coexistence equilibrium when  $\mu_1 = 0, \mu_2 = 0$ . Then, system (2.1) becomes

$$\begin{cases} \frac{\partial u}{\partial t} - d_1 \Delta u = (r_0 + \mu_2)u \left(1 - \frac{u}{K} - \frac{\eta v}{1 + \beta u}\right), & x \in (0, l\pi), t > 0, \\ \frac{\partial v}{\partial t} - (d_{k_0^*}^* + \mu_1) \Delta v = \frac{\gamma(u + \xi)v}{1 + \beta u} - dv - gv^2, & x \in (0, l\pi), t > 0. \end{cases} \tag{3.1}$$

For system (3.1),  $E_* = (u_*, v_*)$  is still the coexistence equilibrium. And considering that Jiang et al. [18] have developed a set of concise formulas of calculating normal form up to order 3 for partial functional differential equations at Turing-Hopf singularity, we utilize these formulas to calculate normal form of system (3.1). Transferring  $E_*$  to the origin, system (3.1) reads

$$\begin{cases} \frac{\partial u}{\partial t} - d_1 \Delta u = (r_0 + \mu_2)(u + u_*) \left(1 - \frac{(u + u_*)}{K} - \frac{\eta(v + v_*)}{1 + \beta(u + u_*)}\right), \\ \frac{\partial v}{\partial t} - (d_{k_0^*}^* + \mu_1) \Delta v = \frac{\gamma((u + u_*) + \xi)(v + v_*)}{1 + \beta(u + u_*)} - d(v + v_*) - g(v + v_*)^2. \end{cases} \tag{3.2}$$

Defining  $U(t) = (u(t); v(t))$ , system (3.2) is written as an abstract differential equation in the phase space  $X$  of the form

$$\frac{dU(t)}{dt} = D(\mu)\Delta U(t) + L(\mu)U(t) + F(U(t), \mu),$$

where

$$D(\mu) = \begin{pmatrix} d_1 & 0 \\ 0 & d_{k_0^*}^* + \mu_1 \end{pmatrix}, \quad L(\mu) = \begin{pmatrix} (r_0 + \mu_2)\alpha_1 & -(r_0 + \mu_2)\beta_1 \\ \alpha_2 & -\beta_2 \end{pmatrix},$$

$$F(\varphi, \mu) = \begin{pmatrix} (r_0 + \mu_2) \left( (\varphi_1 + u_*) \left( 1 - \frac{(\varphi_1 + u_*)}{K} - \frac{\eta(\varphi_2 + v_*)}{1 + \beta(\varphi_1 + u_*)} \right) - (\alpha_1 \varphi_1 - \beta_1 \varphi_2) \right) \\ \frac{\gamma((\varphi_1 + u_*) + \xi)(\varphi_2 + v_*)}{1 + \beta(\varphi_1 + u_*)} - d(\varphi_2 + v_*) - g(\varphi_2 + v_*)^2 - \alpha_2 \varphi_1 + \beta_2 \varphi_2 \end{pmatrix},$$

with  $\varphi = (\varphi_1, \varphi_2)^T \in X$ .

Based on Jiang et al. [18], we attain

$$\begin{aligned} D_0(\mu) &= \begin{pmatrix} d_1 & 0 \\ 0 & d_{k_0^*}^* \end{pmatrix}, & D_1(\mu) &= \begin{pmatrix} 0 & 0 \\ 0 & \mu_1 \end{pmatrix}, \\ L_0(\mu) &= \begin{pmatrix} r_0\alpha_1 & -r_0\beta_1 \\ \alpha_2 & -\beta_2 \end{pmatrix}, & L_1(\mu) &= \begin{pmatrix} \mu_2\alpha_1 & -\mu_2\beta_1 \\ 0 & 0 \end{pmatrix}, \\ Q(\varphi, \varphi) &= \begin{pmatrix} \left( \frac{2r_0\eta\beta v_*}{(1+\beta u_*)^3} - \frac{2r_0}{K} \right) \varphi_1^2 - \frac{2r_0\eta}{(1+\beta u_*)^2} \varphi_1\varphi_2 \\ \frac{2\gamma\beta(\beta\xi-1)v_*}{(1+\beta u_*)^3} \varphi_1^2 - \frac{2\gamma(\beta\xi-1)}{(1+\beta u_*)^2} \varphi_1\varphi_2 - 2g\varphi_2^2 \end{pmatrix}, \\ C(\varphi, \varphi, \varphi) &= \begin{pmatrix} -\frac{6r_0\eta\beta^2 v_*}{(1+\beta u_*)^4} \varphi_1^3 + \frac{6r_0\eta\beta}{(1+\beta u_*)^3} \varphi_1^2\varphi_2 \\ -\frac{6\gamma\beta^2(\beta\xi-1)v_*}{(1+\beta u_*)^4} \varphi_1^3 + \frac{6\gamma\beta(\beta\xi-1)}{(1+\beta u_*)^3} \varphi_1^2\varphi_2 \end{pmatrix}, \end{aligned}$$

with  $\varphi = (\varphi_1, \varphi_2)^T \in X$ . In particular,  $Q(\cdot, \cdot)$  and  $C(\cdot, \cdot, \cdot)$  are determined by the second-order Fréchet and third-order Fréchet derivations of operator  $F(\cdot, 0)$ , respectively. See [18] for more information.

Moreover, the corresponding characteristic matrices are

$$\tilde{\Delta}_k(\lambda) = \begin{pmatrix} \lambda + d_1 \frac{k^2}{l^2} - r_0\alpha_1 & r_0\beta_1 \\ -\alpha_2 & \lambda + d_{k_0^*}^* \frac{k^2}{l^2} + \beta_2 \end{pmatrix}, \quad k \in \mathbb{N}_0.$$

Obviously,  $\lambda = \pm i\omega$  with  $\omega = \sqrt{r_0\Theta}$ , are eigenvalues of  $\tilde{\Delta}_0(0)$ , and  $\lambda = 0$  are a simple eigenvalue for  $\tilde{\Delta}_{k_0^*}(0)$ , with the remaining eigenvalues having negative real parts, according to Theorem 2.3. Then, a direct calculation yields,

$$\begin{aligned} \phi_1 &= \begin{pmatrix} 1 \\ \frac{r_0\alpha_1 l^2 - d_1 k_0^{*2}}{r_0\beta_1 l^2} \end{pmatrix}, & \psi_1 &= \begin{pmatrix} \frac{1}{1 + \frac{(r_0\alpha_1 l^2 - d_1 k_0^{*2})^2}{-r_0\beta_1 \alpha_2 l^4}} \\ \frac{r_0\alpha_1 l^2 - d_1 k_0^{*2}}{-\alpha_2 l^2 \left( 1 + \frac{(r_0\alpha_1 l^2 - d_1 k_0^{*2})^2}{-r_0\beta_1 \alpha_2 l^4} \right)} \end{pmatrix}^T, \\ \phi_2 &= \begin{pmatrix} 1 \\ \frac{r_0\alpha_1 - \omega i}{r_0\beta_1} \end{pmatrix}, & \psi_2 &= \begin{pmatrix} \frac{1}{1 + \frac{(r_0\alpha_1 - \omega i)^2}{-r_0\alpha_2 \beta_1}} \\ \frac{r_0\alpha_1 - \omega i}{-\alpha_2 \left( 1 + \frac{(r_0\alpha_1 - \omega i)^2}{-r_0\alpha_2 \beta_1} \right)} \end{pmatrix}^T. \end{aligned}$$

Furthermore,  $\Phi = (\phi_1, \phi_2, \bar{\phi}_2)$  and  $\Psi = (\psi_1, \psi_2, \bar{\psi}_2)^T$  satisfy  $\psi_1\phi_1 = 1$ , and  $\psi_2\phi_2 = 1$ ,  $\bar{\psi}_2\phi_2 = 0$ .

By [18], normal form restrict on center manifold up to order 3 for reaction-diffusion system (2.1) at Turing-Hopf singularity, is

$$\begin{cases} \dot{z}_1 = a_1(\alpha)z_1 + a_{200}z_1^2 + a_{011}z_2\bar{z}_2 + a_{300}z_1^3 + a_{111}z_1z_2\bar{z}_2 + h.o.t., \\ \dot{z}_2 = i\omega_0z_2 + b_2(\alpha)z_2 + b_{110}z_1z_2 + b_{210}z_1^2z_2 + b_{021}z_2^2\bar{z}_2 + h.o.t., \\ \dot{\bar{z}}_2 = -i\omega_0\bar{z}_2 + \overline{b_2(\alpha)}\bar{z}_2 + \overline{b_{110}z_1z_2} + \overline{b_{210}z_1^2z_2} + \overline{b_{021}z_2^2\bar{z}_2} + h.o.t. \end{cases} \quad (3.3)$$

And, these coefficients  $a_1(\alpha)$ ,  $b_2(\alpha)$ ,  $a_{200}$ ,  $a_{011}$ ,  $a_{300}$ ,  $a_{111}$ ,  $b_{110}$ ,  $b_{210}$ ,  $b_{021}$  could be computed, utilizing formulas provided in Appendix.

### 4. Spatiotemporal patterns with Turing-Hopf bifurcation and discussions

In this section, we show several sets of numerical simulations to support theory analysis. Choosing  $K = 50, \eta = 1, \beta = 0.8, \gamma = 0.4, \xi = 0.3, d = 0.2, g = 0.01, l = 1$ , and diffusion coefficient  $d_1 = 0.01$ , we have  $(u_*, v_*) = (0.4059, 1.3139)$ , which is the unique coexistence equilibrium of system (2.1). And we also derive  $\alpha_1 = 0.2350, \beta_1 = 0.3064, \alpha_2 = 0.2276, \beta_2 = 0.0131$  satisfying  $\alpha_2\beta_1 - \alpha_1\beta_2 > 0$ . Then, the Hopf bifurcation curve in  $d_2$ - $r$  plane is

$$\mathcal{H}_0 : r = r_0 = \frac{\beta_2}{\alpha_1} = 0.0559, \quad d_2 > 0.$$

And, we also have  $k^* = \left\lceil \frac{\beta_2 l^2}{d_1} \right\rceil - 1 = 1$ , and  $k_m = \lfloor \sqrt{x_* l} \rfloor = 1$ . Moreover,  $d_1^* = 1.2290$ , thus  $k_0^* = 1$ , that is,  $k_1 = 1, k_2 = 0$  in Lemma A.1 in Appendix. Then,

$$\begin{aligned} \mathcal{L}_k : r = r_k(d_2) &= \frac{d_1 \left( \beta_2 + d_2 \frac{k^2}{l^2} \right) \frac{k^2}{l^2}}{\alpha_1 \beta_2 - \alpha_2 \beta_1 + \alpha_1 d_2 \frac{k^2}{l^2}} \\ &= \frac{(0.0001314 + 0.01 d_2 k^2) k^2}{-0.06665 + 0.23500 d_2 k^2}, \quad d > d_{2,k}, k \in \mathbb{N}. \end{aligned}$$

Turing bifurcation curves, Hopf bifurcation curve and parameter region of the stability for coexistence equilibrium in  $d_2$ - $r$  plane, are shown in Figure 3.

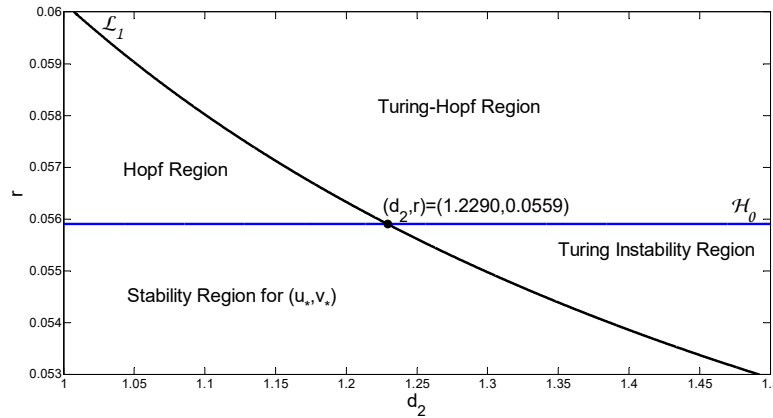


**Figure 3.** Parameter region of the stability for coexistence equilibrium  $E_*$  and global bifurcation set in  $d_2$ - $r$  plane.

Furthermore, for these given parameters, normal form (3.3) for  $(1, 0)$ -mode Turing-Hopf bifurcation truncated to order 3, is

$$\begin{cases} \dot{z}_1 = (0.0025\mu_1 + 0.1793\mu_2) z_1 - 0.0294z_1^3 + 0.0057z_1z_2\bar{z}_2, \\ \dot{z}_2 = (0.1175 + 0.5459i) \mu_2 z_2 - (0.0082 + 0.0250i) z_1^2 z_2 - (0.0027 + 0.1204i) z_2^2 \bar{z}_2, \\ \dot{\bar{z}}_2 = (0.1175 - 0.5459i) \mu_2 \bar{z}_2 - (0.0082 - 0.0250i) z_1^2 \bar{z}_2 - (0.0027 - 0.1204i) \bar{z}_2^2 z_2. \end{cases} \quad (4.1)$$

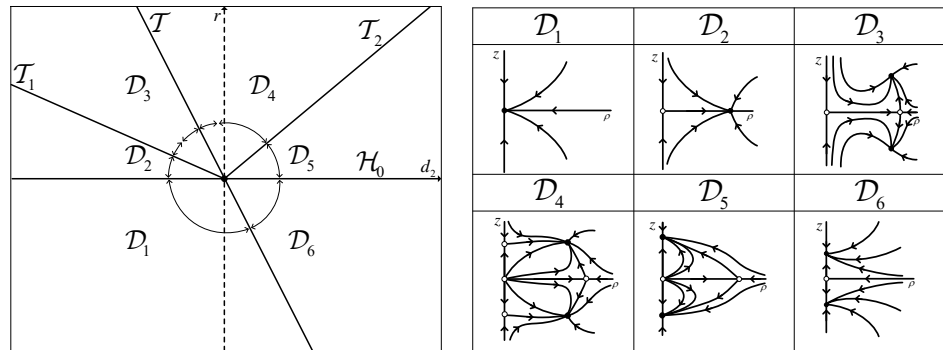
To explore the dynamical behaviors, we consider transformations  $z_1 = z, z_2 = \rho e^{i\theta}, \bar{z}_2 = \rho e^{-i\theta}$ , then system (4.1) is transformed into following amplitude equation,

$$\begin{cases} \dot{z} = (0.0025\mu_1 + 0.1793\mu_2)z - 0.0294z^3 + 0.0057z\rho^2, \\ \dot{\rho} = 0.1175\mu_2\rho - 0.0082\rho z^2 - 0.0027\rho^3. \end{cases} \quad (4.2)$$

According to [12], the unfolding for system (4.2) is Case II. Therefore, define following critical bifurcation curves in  $d_2$ - $r$  plane,

$$\begin{aligned} \mathcal{H}_0 &: r = r_0, & \mathcal{T} &: r = r_0 - 0.01413(d_2 - d_{k_0}^*), \\ \mathcal{T}_1 &: r = r_0 - 0.005929(d_2 - d_{k_0}^*), & d_2 &\leq d_{k_0}^*, \\ \mathcal{T}_2 &: r = r_0 + 0.01047(d_2 - d_{k_0}^*), & d_2 &\geq d_{k_0}^*. \end{aligned}$$

Then, local bifurcation set and phase portraits are shown in Figure 4,



(a) Local bifurcation set of the unfolding Case II of normal form. (b) Phase portraits of the unfolding Case II of normal form.

**Figure 4.** Local bifurcation set (Left) and phase portraits (Right) at Turing-Hopf point  $(d_{k_0}^*, r_0)$ .

**Remark 4.1.** Actually, for normal form of Turing-Hopf bifurcation, there are 12 unfoldings in total, of which each type exhibits different complex dynamics and could reveal different spatiotemporal phenomena, see [12]. As far as we know, the unfolding Case II and corresponding spatiotemporal dynamics have not been discussed before. And, we hope that our discussions could make some contributions to the development of bifurcation theory.

And, local bifurcation set could be embedded in global bifurcation set, see Figure 5. And we find that, near Turing-Hopf bifurcation point, codimension-2 Turing-Hopf bifurcation leads to additional divisions of Hopf region and Turing-Hopf region.

Near Turing-Hopf bifurcation point  $(d_{k_0}^*, r_0)$ , the  $d_2$ - $r$  parameter plane is divided into six regions. And dynamics of system (4.2) are described by corresponding phase portraits respectively, when  $(d_2, r)$  are chosen in these regions. Then based on *normal form method* and *center manifold theory*, we could reveal dynamical behaviors of system (2.1), when parameters are chosen in these six regions, respectively. And we summarize dynamics of system (2.1) as following conclusions.

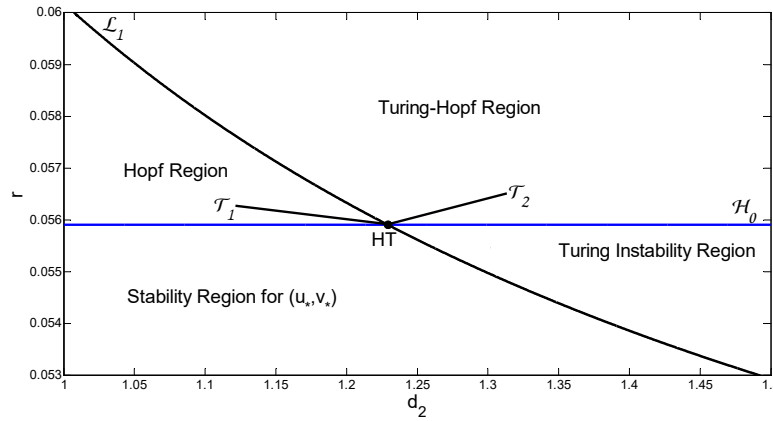


**Figure 5.** Global bifurcation set with local bifurcation curves  $\mathcal{T}_1, \mathcal{T}_2$  at Turing-Hopf bifurcation point  $(d_{k_0}^*, r_0)$ .

**Proposition 4.1.** For fixed parameters  $K = 50, \eta = 1, \beta = 0.8, \gamma = 0.4, \xi = 0.3, d = 0.2, g = 0.01, l = 1, d_1 = 0.01$ , diffusive predator-prey system (2.1) exhibits spatial, temporal and spatiotemporal patterns, when parameters  $(d_2, r)$  are chosen near  $(1, 0)$ -mode Turing-Hopf bifurcation point  $(d_{k_0}^*, r_0) = (1.2290, 0.0559)$ . Here are the results:

1. When  $(d_2, r) \in \mathcal{D}_1$ , the coexistence equilibrium  $E_*$  of system (2.1) is asymptotically stable. Otherwise, the coexistence equilibrium  $E_*$  is unstable when  $(d_2, r) \notin \mathcal{D}_1$ .
2. When  $(d_2, r) \in \mathcal{D}_2$ , system (2.1) has a stable spatially homogeneous periodic solution (see Figure 6), which represents that system exhibits temporal pattern.
3. When  $(d_2, r) \in \mathcal{D}_3$ , there exist a pair of stable spatially inhomogeneous periodic solutions and an unstable spatially homogeneous periodic solution for system (2.1). Thus, system exhibits transient patterns and bistability.
4. When  $(d_2, r) \in \mathcal{D}_4$ , a pair of spatially inhomogeneous steady states and a spatially homogeneous periodic solution for system (2.1) are unstable, and system also has a pair of stable spatially inhomogeneous periodic solutions. Therefore, system exhibits spatiotemporal patterns and bistability (see Figure 7).
5. When  $(d_2, r) \in \mathcal{D}_5$ , there exist an unstable spatially homogeneous periodic solution and a pair of stable spatially inhomogeneous steady states for system (2.1). Hence, system exhibits transient patterns and bistability.
6. When  $(d_2, r) \in \mathcal{D}_6$ , system (2.1) has a pair of stable spatially inhomogeneous steady states (see Figure 8), which indicates that system exhibits spatial patterns and bistability.

Proposition 4.1 indicates that under proper additional food supply to predator and proper intra-specific competition among predator, diffusive predator-prey system (2.1) exhibits complex patterns with temporal period and spatial period, besides spatially inhomogeneous steady states and spatially homogeneous periodic solutions which have been described in [3, 11, 13].

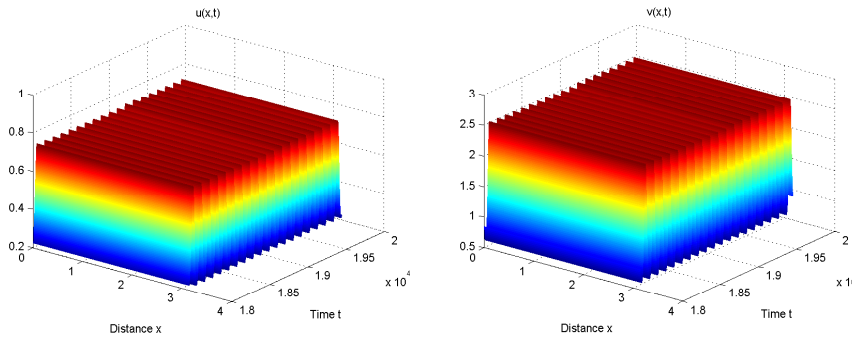


**Figure 6.** For  $(d_2, r) = (1.0290, 0.05690) \in \mathcal{D}_2$ , a spatially homogeneous periodic solution is stable. The initial values are  $u(0, x) = 0.4058560903 + 0.1, v(0, x) = 1.313932244 - 0.2$ .

Next, we briefly discuss the effects of additional food supply to predator and intra-specific competition among predator on dynamics of diffusive system (2.1), respectively.

As we see, intra-specific competition among predator has effects on values and number of coexistence equilibria, according to cubic equation  $h(u)$ . Intra-specific competition among predator could induce three interior equilibria for system (2.1), which might induce more complex spatiotemporal dynamics than these described in Proposition 4.1. Actually, local dynamics near each interior equilibrium are clear, by applying Theorem 2.3 and Lemma A.1 at each interior equilibrium. However, we don't know any more complex global dynamics for predator-prey system (2.1), except local dynamics near each interior equilibrium.

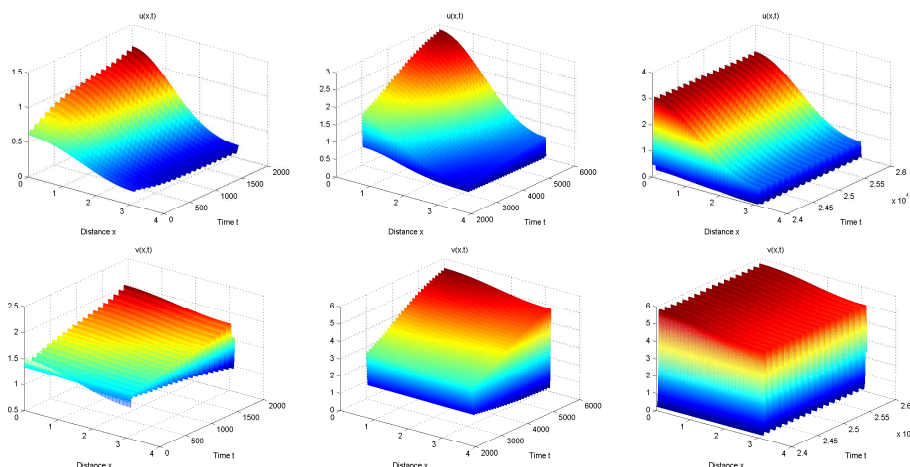
For better understanding, we utilize numerical tools to help discuss the effects of intra-specific competition among predator on dynamics of system (2.1). For given system parameters  $K = 50, \eta = 1, \beta = 0.8, \gamma = 0.4, \xi = 0.3, d = 0.2, l = 1, d_1 = 0.01, d_2 = 1.3290, r = 0.0549$ , the effects of intra-specific competition among predator on the number of coexistence equilibria and on dynamics of diffusive system (2.1) are summarized in Table 1. And, Figure 9 reflects multiple stable coexistence equilibria for system (2.1) at  $g = 0.04$ .

**Table 1.** Effects of intra-specific competition on the number of interior equilibria and long-time dynamics of system (2.1).

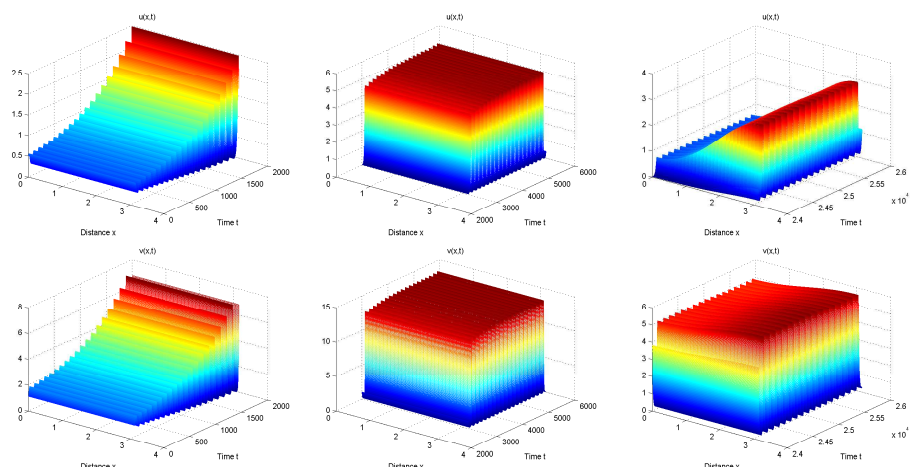
Intra-specific competition $g$	Number	Long-time dynamics
0.005	One	A quasi-periodic solution
0.01, 0.015, 0.02, 0.025	One	A pair of spatial solutions
0.03, 0.04, 0.05, 0.06	Three	A pair of coexistence equilibria
0.065, 0.07, 0.08, 0.1, 0.5	One	A coexistence equilibrium

Numerical simulations show that, proper intra-specific competition among predator induces multiple interior equilibria, which could further induce more complex spatiotemporal dynamics.

As for the effects of additional food supply to predator on dynamics of predator-prey system, it is shown that additional food supply also influences values and number of coexistence equilibria, via destroying assumption (H1). Based on equation



(a) The initial values are  $u(0, x) = 0.4058560903 + 0.2 \cos(x)$ ,  $v(0, x) = 1.313932244 + 0.2 \cos(x)$ .



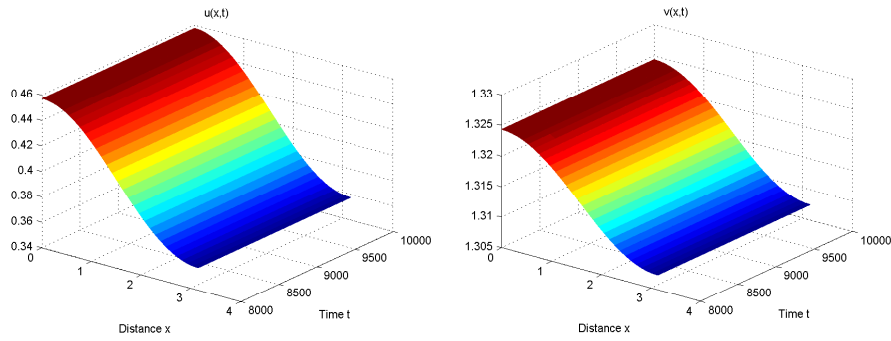
(b) The initial values are  $u(0, x) = 0.4058560903 + 0.1$ ,  $v(0, x) = 1.313932244 - 0.2$ .

**Figure 7.** For  $(d_2, r) = (1.3290, 0.0659) \in \mathcal{D}_4$ , a pair of spatially inhomogeneous periodic solutions are stable. Graphs in the middle reflect transient patterns, which indicate that the spatially homogeneous periodic solution and a pair of spatially inhomogeneous steady states are unstable.

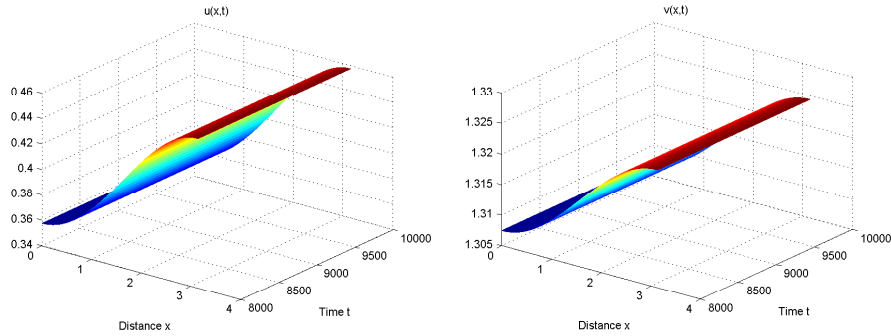
(2.3) and  $h(u)$ , the quantity  $\xi$  of additional food supply has influence on the occurrence of Hopf bifurcation and Turing bifurcation of diffusive system (2.1), and further influences spatiotemporal dynamics of system, via having effects on values of coexistence equilibria. However, it is difficult to theoretically analyze the effects in detail. Instead, we discuss the effects of additional food supply to predator via numerical tools, too.

For given parameters  $K = 50, \eta = 1, \beta = 0.8, \gamma = 0.4, d = 0.2, g = 0.01, l = 1, d_1 = 0.01, d_2 = 1.0290, r = 0.0569$ , the effects of  $\xi$  on the number of coexistence equilibria and dynamics of diffusive system (2.1) are concluded in Table 2. And, Figure 6 and 10 reflect dynamics of system (2.1) when  $\xi = 0.3$  and  $\xi = 0.5$ , respectively.

Numerical simulations show that, proper additional food supply to predator



(a) The initial values are  $u(0, x) = 0.4058560903 + 0.05 \cos(x)$ ,  $v(0, x) = 1.313932244 + 0.05 \cos(x)$ .



(b) The initial values are  $u(0, x) = 0.4058560903 - 0.05 \cos(x)$ ,  $v(0, x) = 1.313932244 - 0.05 \cos(x)$ .

**Figure 8.** For  $(d_2, r) = (1.3290, 0.0549) \in \mathcal{D}_6$ , a pair of spatially inhomogeneous steady states are stable.

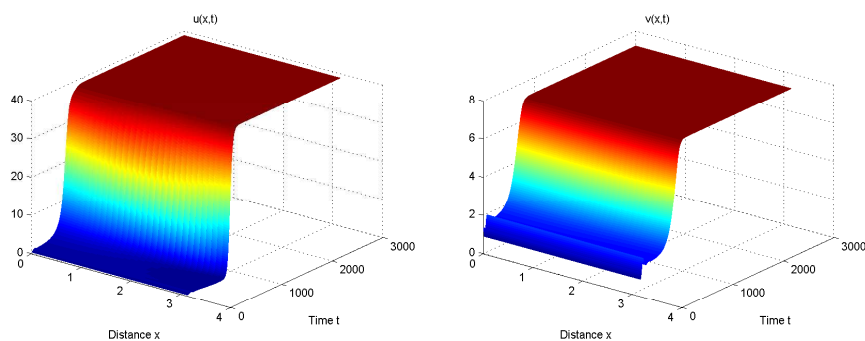
could stabilize steady states of diffusive system (2.1), while large quantity of additional food supply makes interior equilibrium disappear, which indicates that prey becomes extinct and predator changes the source of food.

### 5. Conclusions

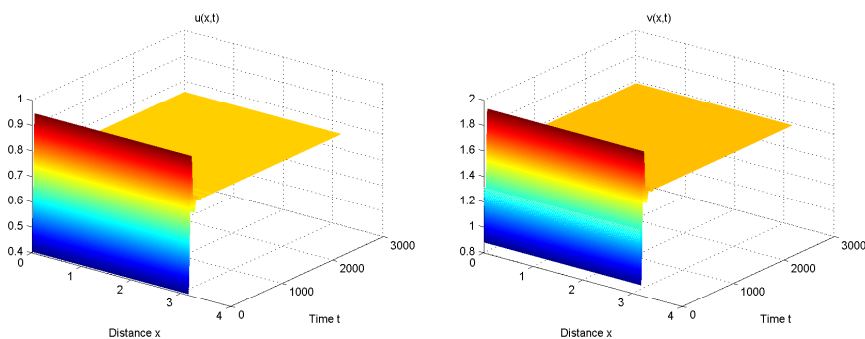
Reaction-diffusion systems could generate complex spatiotemporal patterns via interactions of Turing bifurcation and Hopf bifurcation. In this paper, we explore spatiotemporal dynamics of diffusive predator-prey system (2.1) near Turing-Hopf singularity. It is found that system (2.1) produces interesting spatiotemporal patterns under proper conditions. When parameters are chosen appropriately, system

**Table 2.** Effects of additional food supply on the number of interior equilibria and long-time dynamics of system (2.1).

Quantity of additional food supply $\xi$	Number	Long-time dynamics
0, 0.1, 0.2 0.3	One	A periodic solution
0.4, 0.5	One	A coexistence equilibrium
0.6, 0.7, 0.8,0.9,1	None	Boundary equilibrium $E_2$



(a) The initial values are  $u(0, x) = 0.4058560903 + 0.05 \cos(x)$ ,  $v(0, x) = 1.313932244 + 0.05 \cos(x)$ .



(b) The initial values are  $u(0, x) = 0.4058560903$ ,  $v(0, x) = 1.313932244$ .

**Figure 9.** For intra-specific competition parameter  $g = 0.04$ , there exist multiple stable coexistence equilibria for diffusive system (2.1).

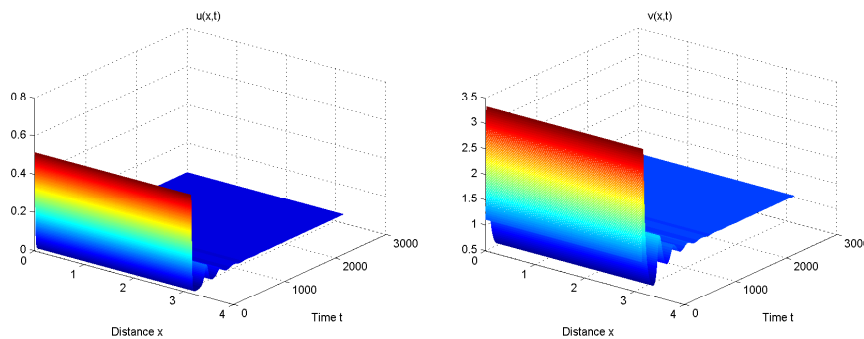


**Figure 10.** For the quantity of additional food supply  $\xi = 0.5$ , spatially homogeneous steady states of diffusive system (2.1) are stable. The initial values are  $u(0, x) = 0.4058560903 + 0.1$ ,  $v(0, x) = 1.313932244 - 0.2$ .

(2.1) exhibits a spatially homogeneous periodic solution, a pair of spatially inhomogeneous steady states and a pair of spatially inhomogeneous periodic solutions, which are induced by Hopf bifurcation, Turing bifurcation and Turing-Hopf bifurcation, respectively.

We also briefly discuss the effects of additional food supply and intra-specific competition on dynamics of diffusive predator-prey system (2.1). Our discussions

show that, intra-specific competition among predator could induce complex spatiotemporal dynamics by inducing multiple coexistence equilibria. Actually, we find that, proper intra-specific competition among predator induce complex patterns which could be used to explain complex natural phenomena, while little intra-specific competition among predator, as well as much intra-specific competition among predator, leads to the loss of complexity in the ecosystem. Much intra-specific competition makes predator spend much time competing with each other, which is benefit for prey, while little intra-specific competition is bad for prey. Similarly, additional food supply to predator also has great influence on the ecosystem. Proper quantity and proper quality of additional food supply to predator could control spatiotemporal chaos and protect the ecosystem, as Ghorai and Porai have stated in [11]. Large quantity and high quality of additional food supply to predator will bring a fatal strike to the ecosystem, since large quantity and high quality of additional food supply to predator makes predator have alternative source of food and leads to the extinction of prey. Once we stop supplying additional food to predator, predator becomes extinct, too. Therefore, too much human intervention will cause collapse of the ecosystem. However, we could supply proper additional food supply to predator to conserve species in an ecosystem.

What's more, we establish conditions of the occurrence of codimension-2 Turing-Turing bifurcation for system (2.1), by further analyzing interactions of Turing bifurcations. And, reaction-diffusion systems might generate some interesting dynamics near Turing-Turing singularity, such as coexisting spatially inhomogeneous steady states with different wavelengths. We anticipate that system (2.1) will produce analogous solutions near Turing-Turing singularity under proper conditions.

## Appendix: calculations of $a_1(\alpha)$ , $b_2(\alpha)$ , $a_{200}$ , $a_{011}$ , $a_{300}$ , $a_{111}$ , $b_{110}$ , $b_{210}$ , $b_{021}$

**Lemma A.1** (See [18]). *For  $k_2 = 0$ ,  $k_1 \neq 0$  and Neumann boundary condition on spatial domain  $\Omega = (0, l\pi)$ ,  $l > 0$ , the parameters  $a_1(\alpha)$ ,  $b_2(\alpha)$ ,  $a_{200}$ ,  $a_{011}$ ,  $a_{300}$ ,  $a_{111}$ ,  $b_{110}$ ,  $b_{210}$ ,  $b_{021}$  in (3.3) are*

$$\begin{aligned} a_1(\alpha) &= \frac{1}{2} \psi_1(0) (L_1(\alpha) \phi_1 - \mu_{k_1} D_1(\alpha) \phi_1(0)), \\ b_2(\alpha) &= \frac{1}{2} \psi_2(0) (L_1(\alpha) \phi_2 - \mu_{k_2} D_1(\alpha) \phi_2(0)), \\ a_{200} &= a_{011} = b_{110} = 0, \\ a_{300} &= \frac{1}{4} \psi_1(0) C_{\phi_1 \phi_1 \phi_1} + \frac{1}{\omega_0} \psi_1(0) \Re(i Q_{\phi_1 \phi_2} \psi_2(0)) Q_{\phi_1 \phi_1} \\ &\quad + \psi_1(0) Q_{\phi_1} \left( h_{200}^0 + \frac{1}{\sqrt{2}} h_{200}^{2k_1} \right), \\ a_{111} &= \psi_1(0) C_{\phi_1 \phi_2 \bar{\phi}_2} + \frac{2}{\omega_0} \psi_1(0) \Re(i Q_{\phi_1 \phi_2} \psi_2(0)) Q_{\phi_2 \bar{\phi}_2} + \\ &\quad \psi_1(0) \left[ Q_{\phi_1} \left( h_{011}^0 + \frac{1}{\sqrt{2}} h_{011}^{2k_1} \right) + Q_{\phi_2} h_{101}^{k_1} + Q_{\bar{\phi}_2} h_{110}^{k_1} \right], \\ b_{210} &= \frac{1}{2} \psi_2(0) C_{\phi_1 \phi_1 \phi_2} + \frac{1}{2i\omega_0} \psi_2(0) \{ 2Q_{\phi_1 \phi_1} \psi_1(0) Q_{\phi_1 \phi_2} \end{aligned}$$

$$\begin{aligned}
 & + [-Q_{\phi_2\phi_2}\psi_2(0) + Q_{\phi_2\bar{\phi}_2}\bar{\psi}_2(0)] Q_{\phi_1\phi_1} \} + \psi_2(0) (Q_{\phi_1}h_{110}^{k_1} + Q_{\phi_2}h_{200}^0) \\
 b_{021} = & \frac{1}{2}\psi_2(0)C_{\phi_2\phi_2\bar{\phi}_2} + \frac{1}{4i\omega_0}\psi_2(0) \left\{ \frac{2}{3}Q_{\bar{\phi}_2\bar{\phi}_2}\bar{\psi}_2(0)Q_{\phi_2\phi_2} \right. \\
 & \left. + [-2Q_{\phi_2\phi_2}\psi_2(0) + 4Q_{\phi_2\bar{\phi}_2}\bar{\psi}_2(0)] Q_{\phi_2\bar{\phi}_2} \right\} + \psi_2(0) (Q_{\phi_2}h_{011}^0 + Q_{\bar{\phi}_2}h_{020}^0). \tag{A.1}
 \end{aligned}$$

where

$$\begin{aligned}
 h_{200}^0(\theta) &= -\frac{1}{2} \left[ \int_{-r}^0 d\eta_0(\theta) \right]^{-1} Q_{\phi_1\phi_1} + \frac{1}{2i\omega_0} (\phi_2(\theta)\psi_2(0) - \bar{\phi}_2(\theta)\bar{\psi}_2(0)) Q_{\phi_1\phi_1}, \\
 h_{200}^{2k_1}(\theta) &\equiv -\frac{1}{2\sqrt{2}} \left[ \int_{-r}^0 d\eta_{2k_1}(\theta) \right]^{-1} Q_{\phi_1\phi_1}, \\
 h_{011}^0(\theta) &= -\left[ \int_{-r}^0 d\eta_0(\theta) \right]^{-1} Q_{\phi_2\bar{\phi}_2} + \frac{1}{i\omega_0} (\phi_2(\theta)\psi_2(0) - \bar{\phi}_2(\theta)\bar{\psi}_2(0)) Q_{\phi_2\bar{\phi}_2}, \\
 h_{011}^{2k_1}(\theta) &= 0, \\
 h_{020}^0(\theta) &= \frac{1}{2} \left[ 2i\omega_0 I - \int_{-r}^0 e^{2i\omega_0\theta} d\eta_0(\theta) \right]^{-1} Q_{\phi_2\phi_2} e^{2i\omega_0\theta} \\
 &\quad - \frac{1}{2i\omega_0} \left[ \phi_2(\theta)\psi_2(0) + \frac{1}{3}\bar{\phi}_2(\theta)\bar{\psi}_2(0) \right] Q_{\phi_2\phi_2}, \\
 h_{110}^{k_1}(\theta) &= \left[ i\omega_0 I - \int_{-r}^0 e^{i\omega_0\theta} d\eta_{k_1}(\theta) \right]^{-1} Q_{\phi_1\phi_2} e^{i\omega_0\theta} - \frac{1}{i\omega_0} \phi_1(0)\psi_1(0) Q_{\phi_1\phi_2}, \\
 h_{002}^0(\theta) &= \overline{h_{020}^0(\theta)}, \quad h_{101}^{k_1}(\theta) = \overline{h_{110}^{k_1}(\theta)}, \tag{A.2}
 \end{aligned}$$

$\theta \in [-r, 0]$ ,  $\phi_1, \phi_2, \psi_1(0), \psi_2(0)$  eigenvectors and dual eigenvectors, see [18, (2.8)], and  $\eta_k \in BV([-r, 0], \mathbb{C}^m)$  is denoted by [18, (2.6)], that is

$$-\mu_k D_0\psi(0) + L_0\psi = \int_{-r}^0 d\eta_k(\theta)\psi(\theta), \quad \psi \in C \triangleq C([-r, 0], \mathbb{C}^m), k \in \mathbb{N}_0. \tag{A.3}$$

**Acknowledgements.** The authors highly appreciate the editors and anonymous reviewers for providing valuable suggestions which helped us to improve the manuscript.

## References

- [1] M. Baurmann, T. Gross and U. Feudel, *Instabilities in spatially extended predator-prey systems: Spatio-temporal patterns in the neighborhood of Turing-Hopf bifurcations*, J. Theoret. Biol., 2007, 245(2), 220–229.
- [2] A. D. Bazykin, A. I. Khibnik and B. Krauskopf, *Nonlinear Dynamics of Interacting Populations*, World Scientific, 1998.
- [3] B. I. Camara, M. Hague and H. Mokrani, *Patterns formations in a diffusive ratio-dependent predator-prey model of interacting populations*, Phys. A, 2016, 461, 374–383.

- [4] S. Chakraborty, P. K. Tiwari, S. K. Sasmal et al., *Interactive effects of prey refuge and additional food for predator in a diffusive predator-prey system*, Appl. Math. Model., 2017, 47, 128–140.
- [5] S. Chen, J. Shi and J. Wei, *Bifurcation analysis of the Gierer-Meinhardt system with a saturation in the activator production*, Appl. Anal., 2013, 93(6), 1115–1134.
- [6] H. Ddumba, J. Y. T. Mugisha, J. W. Gonsalves and G. I. H. Kerley, *Periodicity and limit cycle perturbation analysis of a predator-prey model with interspecific species' interference, predator additional food and dispersal*, Appl. Math. Comput., 2013, 219(15), 8338–8357.
- [7] A. Diouf, H. Mokrani, D. Ngom et al., *Detection and computation of high codimension bifurcations in diffuse predator-prey systems*, Phys. A, 2019, 516, 402–411.
- [8] T. Faria, *Normal forms and hopf bifurcation for partial differential equations with delays*, Trans. Amer. Math. Soc., 2000, 352(5), 2217–2238.
- [9] T. Faria, W. Huang and J. Wu, *Smoothness of center manifolds for maps and formal adjoints for semilinear fdes in general Banach spaces*, SIAM J. Appl. Math., 2002, 34(1), 173–203.
- [10] S. Gakkhar and A. Singh, *Control of chaos due to additional predator in the hastings-powell food chain model*, J. Math. Anal. Appl., 2012, 385(1), 423–438.
- [11] S. Ghorai and S. Poria, *Pattern formation and control of spatiotemporal chaos in a reaction diffusion prey-predator system supplying additional food*, Chaos Solitons Fractals, 2016, 85, 57–67.
- [12] J. Guckenheimer and P. Holmes, *Nonlinear Oscillations, Dynamical Systems, and Bifurcations of Vector Fields*, Springer, New York, 1983.
- [13] L. N. Guin and P. K. Mandal, *Spatiotemporal dynamics of reaction-diffusion models of interacting populations*, Appl. Math. Model., 2014, 38(17–18), 4417–4427.
- [14] S. Guo and J. Man, *Center manifolds theorem for parameterized delay differential equations with applications to zero singularities*, Nonlinear Anal., 2011, 74(13), 4418–4432.
- [15] J. K. Hale, *Theory of Functional Differential Equations*, Springer-Verlag, 1977.
- [16] M. Haque, *A detailed study of the Beddington-Deangelis predator-prey model*, Math. Biosci., 2011, 234(1), 1–16.
- [17] C. S. Holling, *The functional response of predators to prey density and its role in mimicry and population regulation*, Memoirs of the Entomological Society of Canada, 1965, 97(45), 1–60.
- [18] W. Jiang, Q. An and J. Shi, *Formulation of the normal forms of Turing-Hopf bifurcation in reaction-diffusion systems with time delay*, submitted, 2018, arXiv:1802.10286.
- [19] W. Jiang and Y. Yuan, *Bogdanov-Takens singularity in van der pol's oscillator with delayed feedback*, Phys. D, 2007, 227(2), 149–161.
- [20] D. Kumar and S. P. Chakraborty, *A comparative study of bioeconomic ratio-dependent predator-prey model with and without additional food to predators*, Nonlinear Dynam., 2015, 80(1–2), 23–38.

- [21] X. Li, W. Jiang and J. Shi, *Hopf bifurcation and turing instability in the reaction-diffusion Holling-Tanner predator-prey model*, IMA J. Appl. Math., 2011, 78(2), 287–306.
- [22] S. Ma and Z. Feng, *Fold-hopf bifurcations of the Rose-Hindmarsh model with time delay*, Int. J. Bifurc. Chaos, 2011, 21(2), 437–452.
- [23] P. J. Pal, P. K. Mandal and K. K. Lahiri, *A delayed ratio-dependent predator-prey model of interacting populations with Holling type iii functional response*, Nonlinear Dynam., 2014, 76(1), 201–220.
- [24] B. Sahoo and S. Poria, *Effects of additional food on an ecoepidemic model with time delay on infection*, Appl. Math. Comput., 2014, 245, 17–35.
- [25] B. Sahoo and S. Poria, *Effects of additional food in a delayed predator-prey model*, Math. Biosci., 2015, 261, 62–73.
- [26] S. Samanta, R. Dhar, I. M. Elmojtaba and J. Chattopadhyay, *The role of additional food in a predator-prey model with a prey refuge*, J. Biol. Systems, 2016, 24(2–3), 345–365.
- [27] S. Sarwardi, M. Haque and P. K. Mandal, *Persistence and global stability of bazykin predator-prey model with Beddington-Deangelis response function*, Commun. Nonlinear Sci. Numer. Simul., 2014, 19(1), 189–209.
- [28] S. K. Sasmal, Y. Kang and J. Chattopadhyay, *Intra-specific competition in predator can promote the coexistence of an eco-epidemiological model with strong allee effects in prey*, Biosystems, 2015, 137, 34–44.
- [29] M. Sen, P. D. N. Srinivasu and M. Banerjee, *Global dynamics of an additional food provided predator-prey system with constant harvest in predators*, Appl. Math. Comput., 2015, 250, 193–211.
- [30] Y. Song, T. Zhang and Y. Peng, *Turing-Hopf bifurcation in the reaction-diffusion equations and its applications*, Commun. Nonlinear Sci. Numer. Simul., 2016, 33, 229–258.
- [31] Y. Song and X. Zou, *Bifurcation analysis of a diffusive ratio-dependent predator-prey model*, Nonlinear Dynam., 2014, 78(1), 49–70.
- [32] P. D. N. Srinivasu and B. S. R. V. Prasad, *Time optimal control of an additional food provided predator-prey system with applications to pest management and biological conservation*, J. Math. Biol., 2010, 60(4), 591–613.
- [33] Y. Su and X. Zou, *Transient oscillatory patterns in the diffusive non-local blowfly equation with delay under the zero-flux boundary condition*, Nonlinearity, 2014, 27(1), 87–104.
- [34] C. Wang, R. Liu, J. Shi and C. M. Del Rio, *Spatiotemporal mutualistic model of mistletoes and birds*, J. Math. Biol., 2014, 68(6), 1479–1520.
- [35] J. Wang and W. Jiang, *Hopf-zero bifurcation of a delayed predator-prey model with dormancy of predators*, J. Appl. Anal. Comput., 2017, 7(3), 1051–1069.
- [36] J. Wang, J. Wei and J. Shi, *Global bifurcation analysis and pattern formation in homogeneous diffusive predator-prey systems*, J. Differential Equations, 2016, 260(4), 3495–3523.
- [37] S. Wiggins, *Introduction to Applied Nonlinear Dynamical Systems and Chaos*, Springer Science & Business Media, 2003.

- 
- [38] J. Wu, *Theory and Applications of Partial Functional Differential Equations*, Springer, 1996.
- [39] X. Xu and J. Wei, *Turing-Hopf bifurcation of a class of modified Leslie-Gower model with diffusion*, Discrete Contin. Dyn. Syst. Ser. B, 2018, 23(2), 765–783.
- [40] L. Yang, M. Dolnik, A. M. Zhabotinsky and I. R. Epstein, *Spatial resonances and superposition patterns in a reaction-diffusion model with interacting turing modes*, Phys. Rev. Lett., 2002, 88(20).
- [41] R. Yang and Y. Song, *Spatial resonance and turing-hopf bifurcations in the Gierer-Meinhardt model*, Nonlinear Anal. Real World Appl., 2016, 31, 356–387.
- [42] R. Z. Yang, M. Liu and C. R. Zhang, *A delayed-diffusive predator-prey model with a ratio-dependent functional response*, Commun. Nonlinear Sci. Numer. Simul., 2017, 53, 94–110.
- [43] F. Yi, J. Wei and J. Shi, *Bifurcation and spatiotemporal patterns in a homogeneous diffusive predator-prey system*, J. Differential Equations, 2009, 246(5), 1944–1977.
- [44] R. Yuan, W. Jiang and Y. Wang, *Saddle-node-hopf bifurcation in a modified leslie-gower predator-prey model with time-delay and prey harvesting*, J. Math. Anal. Appl., 2015, 422(2), 1072–1090.
- [45] T. Zhang, X. Liu, X. Meng and T. Zhang, *Spatio-temporal dynamics near the steady state of a planktonic system*, Comput. Math. Appl., 2018, 75(12), 4490–4504.